UNIVERSITY OF BIRMINGHAM
University of Birmingham Research at Birmingham

Measurement of the energy response of the ATLAS calorimeter to charged pions from $W^{\pm} \to \tau^{\pm}(\to \pi^{\pm}\nu_{\tau})\nu_{\tau}$ events in Run 2 data

ATLAS Collaboration; Newman, Paul

DOI:
10.1140/epjc/s10052-022-10117-2

License:
Creative Commons: Attribution (CC BY)

Document Version
Publisher's PDF, also known as Version of record

Citation for published version (Harvard):
ATLAS Collaboration & Newman, P 2022, 'Measurement of the energy response of the ATLAS calorimeter to charged pions from $W^{\pm} \to \tau^{\pm}(\to \pi^{\pm}\nu)\nu$ events in Run 2 data', *European Physical Journal C*, vol. 82, no. 3, 223. https://doi.org/10.1140/epjc/s10052-022-10117-2

Link to publication on Research at Birmingham portal

General rights
Unless a licence is specified above, all rights (including copyright and moral rights) in this document are retained by the authors and/or the copyright holders. The express permission of the copyright holder must be obtained for any use of this material other than for purposes permitted by law.

•Users may freely distribute the URL that is used to identify this publication.
•Users may download and/or print one copy of the publication from the University of Birmingham research portal for the purpose of private study or non-commercial research.
•User may use extracts from the document in line with the concept of 'fair dealing' under the Copyright, Designs and Patents Act 1988 (?)
•Users may not further distribute the material nor use it for the purposes of commercial gain.

Where a licence is displayed above, please note the terms and conditions of the licence govern your use of this document.

When citing, please reference the published version.

Take down policy
While the University of Birmingham exercises care and attention in making items available there are rare occasions when an item has been uploaded in error or has been deemed to be commercially or otherwise sensitive.

If you believe that this is the case for this document, please contact UBIRA@lists.bham.ac.uk providing details and we will remove access to the work immediately and investigate.

Download date: 20. Apr. 2024

Eur. Phys. J. C (2022) 82:223
https://doi.org/10.1140/epjc/s10052-022-10117-2

THE EUROPEAN PHYSICAL JOURNAL C

Regular Article - Experimental Physics

Measurement of the energy response of the ATLAS calorimeter to charged pions from $W^{\pm} \to \tau^{\pm}(\to \pi^{\pm}\nu_{\tau})\nu_{\tau}$ events in Run 2 data

ATLAS Collaboration[⋆]

CERN, 1211 Geneva 23, Switzerland

Received: 23 August 2021 / Accepted: 10 February 2022
© CERN for the benefit of the ATLAS collaboration 2022

Abstract The energy response of the ATLAS calorimeter is measured for single charged pions with transverse momentum in the range $10 < p_{\mathrm{T}} < 300$ GeV. The measurement is performed using 139 fb^{-1} of LHC proton–proton collision data at $\sqrt{s} = 13$ TeV taken in Run 2 by the ATLAS detector. Charged pions originating from τ-lepton decays are used to provide a sample of high-p_{T} isolated particles, where the composition is known, to test an energy regime that has not previously been probed by in situ single-particle measurements. The calorimeter response to single-pions is observed to be overestimated by ∼2% across a large part of the p_{T} spectrum in the central region and underestimated by ∼4% in the endcaps in the ATLAS simulation. The uncertainties in the measurements are $\lesssim$1% for $15 < p_{\mathrm{T}} < 185$ GeV in the central region. To investigate the source of the discrepancies, the width of the distribution of the ratio of calorimeter energy to track momentum, the energies per layer and response in the hadronic calorimeter are also compared between data and simulation.

Contents

1 Introduction . . . .
2 ATLAS detector . . . .
3 Data and samples of simulated events . . . .
4 Event selection, observables and response extraction .
5 Calorimeter response measurement and comparison with simulation . . . .
6 Uncertainties in the response measurement . . . .
7 Width of the $E_{\mathrm{T}}^{\mathrm{EM}}/p_{\mathrm{T}}^{\mathrm{trk}}$ distribution . . . .
8 Measurements of the longitudinal energy profile and late showering particles . . . .
9 Conclusion . . . .
References . . . .

1 Introduction

The energetic proton–proton (pp) collisions produced by the Large Hadron Collider (LHC) predominantly result in a large number of charged and neutral hadrons which form collimated sprays known as jets. In the ATLAS Experiment [1] the energy of these particles is measured using the calorimeters, and a tracking system measures the momentum of the charged particles. A particle-flow algorithm [2] is used to take advantage of these two systems in the reconstruction of jets. The measurement of hadronic energy deposits is essential for the reconstruction of jets and the jet energy scale calibration relies on the accurate simulation of hadrons interacting with the calorimeter [3]. A powerful method of understanding the calorimeter response to hadrons is to consider the ratio of the energy reconstructed in the calorimeter to the momentum measured in the well-aligned tracking detector [4]. Previously, this was studied using isolated single hadrons from inclusive pp collisions [5,6]. In this paper, the large dataset accumulated in Run 2 is exploited to select events with isolated charged pions from τ-lepton decays so that a much higher energy regime can be probed.

The calorimeter response to electromagnetic particles such as electrons and photons is very well known due to their showers being easier to simulate accurately and precise measurements in situ using $Z \to ee$ events. The energy scale of electrons is therefore known with an uncertainty of less than 0.1% for transverse momenta $25 < p_{\mathrm{T}} < 70$ GeV in the central region [7]. The large variety of physics processes in hadronic interactions and the non-compensating nature of the ATLAS calorimeters make the response to hadrons harder to model in simulation, motivating in situ measurements using highly energetic single pions from τ-lepton decays.

In this paper the calorimeter response across a wide range of transverse momenta is investigated. W bosons are produced copiously at the LHC and can decay via τ-leptons to single charged pions, providing a source of isolated pions: $W^{\pm} \to \tau^{\pm}(\to \pi^{\pm}\nu_{\tau})\nu_{\tau}$. Using the Run 2 dataset recorded in 2015–2018, large samples of pions are selected in order to

⋆ e-mail: atlas.publications@cern.ch

Published online: 14 March 2022

accurately measure the calorimeter response using the ratio of calorimeter energy to track momentum. The measured response is corrected for the contributions from the multiple pp interactions per bunch crossing and the residual signals remaining in the calorimeter from adjacent bunch crossings, contributions collectively referred to as *pile-up*. The charged-pion response is measured as a function of track pseudorapidity, η^{trk}, across the tracker volume and as a function of track transverse momentum, $p_{\text{T}}^{\text{trk}}$, in the barrel and endcaps. The average particle energy in the highest $p_{\text{T}}^{\text{trk}}$ bin in the endcaps is 680 (670) GeV in data (simulated data).

Previous measurements of the single-hadron response using this ratio were performed using 2010 and 2012 data [5,6]. These measurements focused on special runs with low instantaneous luminosity and identified isolated tracks from minimum-bias events. As high-momentum isolated tracks are not frequently produced in pure QCD interactions due to the formation of jets which consist of multiple closely spaced particles, they probed the low-momentum phase space with $p < 30$ GeV. Test-beam measurements using the Super Proton Synchrotron (SPS) probed the response to hadrons with energies, E, up to 350 GeV [8–12]. For the combined, electromagnetic and hadronic, barrel calorimeter, the precision of these measurements ranged from 2.8% at $E = 20$ GeV to 1.4% at $E = 350$ GeV [12]. The uncertainties were dominated by the non-uniformity of the calorimeter, imperfect knowledge of the effect of the material in front of it, and, for positive beams, the fraction of protons. In this paper the response is measured in situ with a pure $\pi^{\pm}$ sample. Additionally, the latest ATLAS detector simulation with updated geometry [13] and with the latest set of hadronic shower simulation models (called the *physics list* [14]) as used in all recent physics analyses, is used in the comparisons of data with simulation.

Precise knowledge of the calorimeter response at high p_{T} is essential for many ATLAS physics analyses. The uncertainty in the energy scale calibration of hadronic jets, the jet energy scale (JES) [3], is one of the primary experimental uncertainties in many searches for new physics and in measurements of Standard Model processes [15–18]. In situ techniques are used to derive corrections to the transverse momentum of jets to account for differences between data and simulation, as well as uncertainties in these corrections. For the highest-p_{T} jets in the TeV regime, where in situ methods exploiting p_{T} balance cannot be used due to a lack of data because of the low cross-section, the determination of the uncertainties in the momentum relies on measurements of the calorimeter energy scale from single hadrons. These are based on the low-momentum in situ measurements, test-beam results and conservative extrapolations, further motivating this measurement. Also, the calibration of hadronically decaying τ-leptons relies on these measurements at high p_{T} [19]. Additionally, measurements of the internal structure of jets rely on knowledge of the calorimeter energy scale [20]. Likewise, when tagging hadronically decaying heavy particles [21] the jet substructure variables that are used cannot be corrected easily for calorimeter scale discrepancies, so they depend on good modelling of the underlying calorimeter energy scale.

The paper is organised as follows. Section 2 introduces the ATLAS detector, and Sect. 3 describes the dataset and samples of simulated events. The selection of events for the measurement and the variable of interest are defined in Sect. 4. The energy response is evaluated in Sect. 5 and uncertainties in the measurements are evaluated in Sect. 6. The width of the distribution of the variable of interest is measured in Sect. 7 and the longitudinal segmentation of the calorimeters is exploited in Sect. 8 to investigate discrepancies between simulation and data. Finally, the conclusions are presented in Sect. 9.

2 ATLAS detector

The ATLAS experiment [1,22,23] at the LHC is a multipurpose particle detector with a forward–backward symmetric cylindrical geometry and a near 4π coverage in solid angle.[1] It consists of an inner tracking detector surrounded by a thin superconducting solenoid providing a 2 T axial magnetic field, electromagnetic and hadronic calorimeters, and a muon spectrometer.

The inner tracking detector covers the pseudorapidity range $|\eta| < 2.5$. Radially outwards, it consists of silicon pixel, silicon microstrip, and transition radiation tracking (TRT) detectors.

Lead/liquid-argon (LAr) sampling calorimeters provide electromagnetic (EM) energy measurements with high granularity. A central barrel covers $|\eta| < 1.475$ and endcaps cover $1.375 < |\eta| < 3.2$. A steel/scintillator-tile (Tile) hadron calorimeter covers the central pseudorapidity range with one barrel covering $|\eta| < 1$ and extended barrels also covering $0.8 < |\eta| < 1.7$. These are longitudinally segmented in shower depth into three layers. Hadronic calorimetry in the endcaps (HEC) is provided by a copper/liquid-argon calorimeter which consists of four layers. The forward regions are instrumented with LAr calorimeters for both the EM and hadronic energy measurements up to $|\eta| =$

[1] ATLAS uses a right-handed coordinate system with its origin at the nominal interaction point (IP) in the centre of the detector and the z-axis along the beam pipe. The x-axis points from the IP to the centre of the LHC ring, and the y-axis points upwards. Polar coordinates (r, ϕ) are used in the transverse plane, ϕ being the azimuthal angle around the z-axis. The pseudorapidity is defined in terms of the polar angle θ as $\eta = -\ln\tan(\theta/2)$. Angular distance is measured in units of $\Delta R \equiv \sqrt{(\Delta\eta)^2 + (\Delta\phi)^2}$.

4.9. Additionally pre-sampler and crack scintillators recover energy lost in non-instrumented regions.

The muon spectrometer surrounds the calorimeters and is based on three large air-core toroidal superconducting magnets with eight coils each. The field integral of the toroids ranges between 2.0 and 6.0 T m across most of the detector. The muon spectrometer includes a system of precision tracking chambers and fast detectors for triggering.

A two-level trigger system is used to select events [24]. The first-level trigger is implemented in hardware and uses a subset of the detector information to accept events at a rate below 100 kHz. This is followed by a software-based trigger that reduces the accepted event rate to 1 kHz on average, depending on the data-taking conditions.

An extensive software suite [25] is used for real and simulated data reconstruction and analysis, for operation and in the trigger and data acquisition systems of the experiment.

3 Data and samples of simulated events

The pp collision data analysed were recorded with the ATLAS detector from 2015 to 2018 at a centre-of-mass energy, $\sqrt{s}$, of 13 TeV. The average number of pp interactions per bunch crossing was 33.7[2] and it varied from $\approx$ 10 to $\approx$ 65. Events were selected by missing transverse momentum ($E_{\mathrm{T}}^{\mathrm{miss}}$) triggers [27]. After the application of data-quality requirements [28], the data sample corresponds to an integrated luminosity of 139 fb^{-1} with an uncertainty of 1.7% [26] obtained using the LUCID-2 detector [29] for the primary luminosity measurements.

Samples of simulated events created using Monte Carlo techniques are used to model the Standard Model processes. The main signal processes are $W(\rightarrow \tau\nu_\tau)$+jets and top pair production ($t\bar{t}$), with smaller signal contributions from single top production and small background contributions from $W(\rightarrow e\nu_e, \mu\nu_\mu)$+jets and $Z(\rightarrow \nu\nu)$+jets. Other processes are cross-checked with simulated event samples and found to be negligible.

The production of W+jets and Z+jets was simulated with the Sherpa 2.2.1 [30,31] generator using matrix elements (MEs) with next-to-leading-order (NLO) accuracy for up to two jets, and matrix elements with leading-order accuracy for up to four jets, calculated with the Comix [32] and OpenLoops [33,34] libraries. They were matched with the Sherpa parton shower [35] using the MEPS@NLO prescription [36–39] with the set of tuned parameters (tune) developed by the Sherpa authors. All polarisation effects in τ-lepton production were retained by using a full matrix element calculation, and were propagated to its decay in the HADRONS++ module, which implements intermediate hadronic resonances and spin-correlation effects. The NNPDF3.0nnlo set of parton distribution functions (PDFs) [40] was used and the samples are normalised to a next-to-next-to-leading-order (NNLO) prediction [41].

The production of $t\bar{t}$ and single-top-quark events was modelled using the Powheg Box v2 [42–45] generator at NLO with the NNPDF3.0nlo [40] set of PDFs. These events were processed with Pythia 8.230 [46] using the A14 tune [47] and the NNPDF2.3lo set of PDFs [48]. The decays of bottom and charm hadrons were modelled using the EvtGen 1.6.0 [49] program. In $t\bar{t}$ events the h_{damp} parameter[3] was set to $1.5\,m_{\mathrm{top}}$ [50]. The $t\bar{t}$ process is normalised to the inclusive cross-section calculation at NNLO in QCD including the resummation of next-to-next-to-leading logarithmic (NNLL) soft-gluon terms from Top++2.0 [51–57]. The single-top-quark production processes are normalised to the inclusive cross-sections calculated at NLO in QCD with NNLL soft-gluon corrections [58,59]. For single top quark production in the Wt-channel events, the diagram removal scheme [60] was used to remove overlap with $t\bar{t}$ production. In all samples the top quark mass is 172.5 GeV.

To study the generator dependence of the analysis an alternative sample of QCD W+jets events was simulated by MadGraph5_aMC@NLO 2.2.2 [61] using LO-accurate MEs with up to four final-state partons and the NNPDF3.0nlo set of PDFs. The events were interfaced to Pythia 8.186 [62], with the A14 tune using the NNPDF2.3lo PDF set, for the modelling of the parton shower, hadronisation, and underlying event. The overlap between matrix element and parton shower emissions was removed using the CKKW-L merging procedure [63,64]. The decays of bottom and charm hadrons were performed by EvtGen 1.2.0 [49].

All samples were passed through a detailed simulation of the ATLAS detector [65] based on Geant4 [66]. The modelling of hadron interactions was done by the `FTFP_BERT_ATL` [14] physics list. In this physics list the *Bertini cascade model* [67] is used for hadrons with energy below 12 GeV, and the *Fritiof string model* [68,69] for hadrons with energy above 9 GeV. The probability of using each model changes smoothly across the region of overlap.

Furthermore, simulated inclusive inelastic pp collisions were overlaid to model additional pile-up collisions in the same and neighbouring bunch crossings. These were generated with Pythia 8.210 [46] with the A3 tune [70] and NNPDF2.3lo PDF set.

[2] The average number of pp interactions per bunch crossing is calculated in data using the instantaneous per bunch luminosity [26] and a reference inelastic cross section which we take to be 80 mb.

[3] The h_{damp} parameter is a resummation damping factor and one of the parameters that controls the matching of Powheg matrix elements to the parton shower and thus effectively regulates the high-p_{T} radiation against which the $t\bar{t}$ system recoils.

4 Event selection, observables and response extraction

Events are selected using the properties of reconstructed objects to obtain a high-purity sample of $W^{\pm} \to \tau^{\pm}(\to \pi^{\pm}\nu_{\tau})\nu_{\tau}$ decays which are used to measure the calorimeter response. The calorimeter energy associated with the track is summed and a fit to the energy divided by the track momentum is performed to extract the calorimeter response. The reconstructed objects used to form the variable of interest are described as follows:

- Charged-pion tracks are reconstructed by an iterative track-finding algorithm seeded by measurements in the silicon layers of the inner detector [71,72]. The precise alignment of the inner detector ensures that these tracks are accurately reconstructed with a residual sagitta bias and momentum scale bias of less than 0.1 TeV^{-1} and 0.9×10^{-3} respectively [4].
- *Calorimeter topoclusters* are clusters of connected calorimeter cells throughout both the EM and hadronic calorimeters. They are seeded from cells with reconstructed energy significantly above the noise [73]. Their energy is the sum of the energies of the constituent cells, which are calibrated at the electromagnetic scale. This scale is defined such that the response to electromagnetic showers is correctly calibrated in all calorimeters. Due to the non-compensating nature of the ATLAS calorimeters, the response to hadronic showers is expected to be lower such that they will be under-calibrated. Single particles can form multiple topoclusters [2], so when measuring the response all clusters in both the EM and hadronic calorimeters within a region are summed.

Additionally, various other reconstructed particles and observables are used in the event selection:

- Electrons are reconstructed from tracks and calorimeter energy deposits. They are identified through a log-likelihood discriminant based on the track properties and the shower shape in the calorimeter. Electrons are identified with the *Loose* working point and require $p_{\text{T}} > 10$ GeV and $|\eta| < 2.47$ [74].
- Muons are reconstructed using combined fits of inner detector and muon spectrometer tracks and are required to meet the *Medium* identification criteria and have $p_{\text{T}} > 10$ GeV and $|\eta| < 2.7$ [75]. The momentum scale and resolution for muons are precisely calibrated and measured using the Z-boson and J/ψ resonances [76].
- Jets are reconstructed for the purpose of building the missing transverse momentum, $E_{\text{T}}^{\text{miss}}$. Particle-flow objects [2] are clustered using the anti-k_t algorithm [77] with radius parameter $R = 0.4$ using the FastJet package [78] and are calibrated to the scale of jets built from the momentum of the stable interacting particles entering the simulation using the same algorithm. During the calibration sequence, corrections are applied to mitigate the effects of pile-up, and jets in data are corrected for residual differences between data and simulation measured in situ using various p_{T}-balance techniques [3]. Calibrated jets are required to have $p_{\text{T}} > 20$ GeV. Jets originating from pile-up are rejected using inner-detector information [79].
- $E_{\text{T}}^{\text{miss}}$ is reconstructed from the vector sum of the momenta of the *hard objects* described above and a *soft term* formed from tracks matched to the primary vertex (PV)[4] of interest but not associated with any *hard object* [81].

The event selection is based on the above reconstructed particles and observables, and is designed to obtain a high-purity sample of $W^{\pm} \to \tau^{\pm}(\to \pi^{\pm}\nu_{\tau})\nu_{\tau}$ events with the following properties:

1. $E_{\text{T}}^{\text{miss}} > 150$ GeV in addition to being selected by the missing transverse momentum trigger.
2. A leading track with $p_{\text{T}} > 10$ GeV and $|\eta| < 2.5$ satisfying the following criteria:
   - The sum of the p_{T} of other tracks, matched to the PV, within a cone of size $\Delta R = 0.3$ around the track is less than 2 GeV.
   - The track's longitudinal impact parameter, measured relative to the PV, is less than 1.5 mm.
   - The track's transverse impact parameter, measured relative to the beamline, is less than 0.5 mm.
   - The track satisfies the *tight* criteria for hits in the silicon pixel and microstrip detectors [82].
   - The χ^2 per degree of freedom of the track fit is less than 1.5.
   - Several TRT hits are used in the track fit if the track is within $|\eta| < 2.0$.
3. There are no reconstructed electrons or muons within $\Delta R = 0.4$ of the leading track.
4. At least 15% of the total energy of all topoclusters within $\Delta R = 0.15$ of the track is deposited in the hadronic calorimeters.
5. There are less than two muon spectrometer track segments [75] within $\Delta R = 0.15$ of the track.
6. The track does not point at any region of the Tile calorimeter that had defects during that time period.

[4] The primary vertex is the reconstructed vertex [80] with the highest summed p_{T}^2 of tracks associated with it.

7. To reduce backgrounds where the reconstructed track is not from $W^{\pm} \to \tau^{\pm}(\to \pi^{\pm}\nu_{\tau})\nu_{\tau}$, the transverse mass[5] of the leading track and the $E_{\mathrm{T}}^{\mathrm{miss}}$ satisfies $m_{\mathrm{T}} < 100$ GeV, or $m_{\mathrm{T}} < 90$ GeV if $p_{\mathrm{T}}^{\mathrm{trk}} < 30$ GeV, or $m_{\mathrm{T}} < 80$ GeV if $p_{\mathrm{T}}^{\mathrm{trk}} < 20$ GeV.
8. The transverse impact parameter of the track relative to the beamline is greater than: 0.04 mm if $p_{\mathrm{T}}^{\mathrm{trk}} < 16$ GeV, 0.03 mm if $16 < p_{\mathrm{T}}^{\mathrm{trk}} < 20$ GeV, and 0.02 mm if $20 < p_{\mathrm{T}}^{\mathrm{trk}} < 30$ GeV. No criteria is applied to tracks with $p_{\mathrm{T}}^{\mathrm{trk}} > 30$ GeV. This exploits the lifetime of the τ-lepton to reduce backgrounds where the track is from a QCD process.

The first criterion ensures that the selected events are in the well-understood region of the $E_{\mathrm{T}}^{\mathrm{miss}}$ trigger efficiency where it is not rapidly changing with respect to $E_{\mathrm{T}}^{\mathrm{miss}}$. The tracking criteria select isolated tracks associated with the primary vertex that have a large number of hits to measure the momentum. The TRT hit requirements and the criterion for the χ^2 per degree of freedom of the track fit ensure that the track reconstruction uses the large lever arm within the TRT volume and that the track fit is of good quality. The third, fourth and fifth criteria reject tracks that are formed from electrons, muons and converted photons. The final two criteria reject events where the track does not originate from a τ-lepton; such backgrounds are only significant at low $p_{\mathrm{T}}^{\mathrm{trk}}$. They utilise the expected displacement of the track owing to the τ-lepton lifetime and the expected upper bound on the transverse mass at the W boson mass.

After this selection the sample has a high purity of $W^{\pm} \to \tau^{\pm}(\to \pi^{\pm} + \nu_{\tau})\nu_{\tau}$ events with the most significant background being $W^{\pm} \to \tau^{\pm}(\to \pi^{\pm} + n\pi^0 + \nu_{\tau})\nu_{\tau}$ events. For each track the transverse energy of the clusters within a fixed cone with $\Delta R = 0.15$ of the track, taking into account the effect of the magnetic field, is summed. The ratio of this summed transverse energy of all clusters, in all calorimeters, at the electromagnetic scale to the track p_{T} forms the variable of interest, $E_{\mathrm{T}}^{\mathrm{EM}}/p_{\mathrm{T}}^{\mathrm{trk}}$. Based on the simulation, it is not expected that the event selection will bias the response significantly and the selection criteria are varied to check that the results of the analysis are not sensitive to the specific selection criteria.

The summed calorimeter energy deposit is corrected for pile-up contributions. Following the methodology used in the calibration of jets, the measured median p_{T} density in the y–ϕ plane of the event, ρ [3,83], scaled by the area of the cone within which we sum clusters, $A = \pi \times 0.15^2$, is subtracted. After this subtraction there is a small residual pile-up dependence which is subtracted using the average number of interactions per bunch crossing, μ^{PU}, and the gradient, α, determined from simulation as a function of $|\eta|$: $\alpha(|\eta|) \times \mu^{\mathrm{PU}}$. Only one residual correction is applied compared to two in the calibration of jets as the pile-up contributions are much smaller in this case due to the smaller area considered. This methodology is different from the previous single-hadron response measurement in a low pile-up environment [5,6], where pile-up and physics backgrounds were both subtracted. In this analysis the pile-up is subtracted but the physics background is included in the functional fit.

Events are selected according to their $p_{\mathrm{T}}^{\mathrm{trk}}$ and $|\eta^{\mathrm{trk}}|$ values to probe the different regions of phase space. Figure 1 shows the distribution of the variable of interest, $E_{\mathrm{T}}^{\mathrm{EM}}/p_{\mathrm{T}}^{\mathrm{trk}}$, for six of the $(p_{\mathrm{T}}^{\mathrm{trk}}, |\eta^{\mathrm{trk}}|)$ bins. Due to differences in the $E_{\mathrm{T}}^{\mathrm{EM}}/p_{\mathrm{T}}^{\mathrm{trk}}$ scale and resolution between simulation and data, some clear discrepancies are seen in the data-to-MC ratio.

The primary background is from events with τ-leptons which decay to a charged pion, $\pi^{\pm}$, and at least one neutral pion, π^0. In the calorimeter, more energy will be reconstructed from this process for the same track momentum due to the electromagnetic shower from the π^0, which predominantly decays as $\pi^0 \to \gamma\gamma$. This results in an upper tail in the $E_{\mathrm{T}}^{\mathrm{EM}}/p_{\mathrm{T}}^{\mathrm{trk}}$ distribution. Other single-charged-particle τ-lepton decays, such as $\tau^{\pm} \to K^{\pm}\nu_{\tau}$, also contribute at a lower level.

The aim of this analysis is to extract the mean and width of a Gaussian function fitted to the $W^{\pm} \to \tau^{\pm}(\to \pi^{\pm}\nu_{\tau})\nu_{\tau}$ signal in the core of the $E_{\mathrm{T}}^{\mathrm{EM}}/p_{\mathrm{T}}^{\mathrm{trk}}$ distribution to probe the calorimeter response and resolution. To extract this, the distribution is fit with the sum of a Gaussian function and another function that describes the background from all processes other than $W^{\pm} \to \tau^{\pm}(\to \pi^{\pm}\nu_{\tau})\nu_{\tau}$. The functional form of this second term is taken to be a *Landau* function [84]. This is chosen empirically as it is seen to accurately capture the shape of the background. The range of the fit is then taken as the mean, $\mu_{\pi^{\pm}}$, of a Gaussian function describing $E_{\mathrm{T}}^{\mathrm{EM}}/p_{\mathrm{T}}^{\mathrm{trk}}$ for signal in simulation minus 1.5 times its width, $\sigma_{\pi^{\pm}}$, to 2, i.e. $[(\mu_{\pi^{\pm}} - 1.5\sigma_{\pi^{\pm}}), 2]$. The combined Gaussian+Landau function is fit to the distribution in data and simulation. In both cases the shape of the Landau function is fixed from a fit to the background processes in simulation. The three parameters of the Gaussian signal and the normalisation of the Landau function are allowed to float in the final fit. The mean of the Gaussian function gives the calorimeter response scale and the width of the Gaussian function measures the resolution of $E_{\mathrm{T}}^{\mathrm{EM}}/p_{\mathrm{T}}^{\mathrm{trk}}$, which contains components from both the calorimeter and track reconstruction. Figure 1 shows the functions fitted to data and simulation in six of the $(p_{\mathrm{T}}^{\mathrm{trk}}, |\eta^{\mathrm{trk}}|)$ bins, and the extracted mean and width of the Gaussian function are displayed.

[5] The transverse mass is defined by $m_{\mathrm{T}} = \sqrt{2p_{\mathrm{T}}^{\mathrm{trk}}E_{\mathrm{T}}^{\mathrm{miss}}[1 - \cos(\Delta\phi)]}$, where $\Delta\phi$ is the angle in the azimuthal plane between the $E_{\mathrm{T}}^{\mathrm{miss}}$ direction and the track.

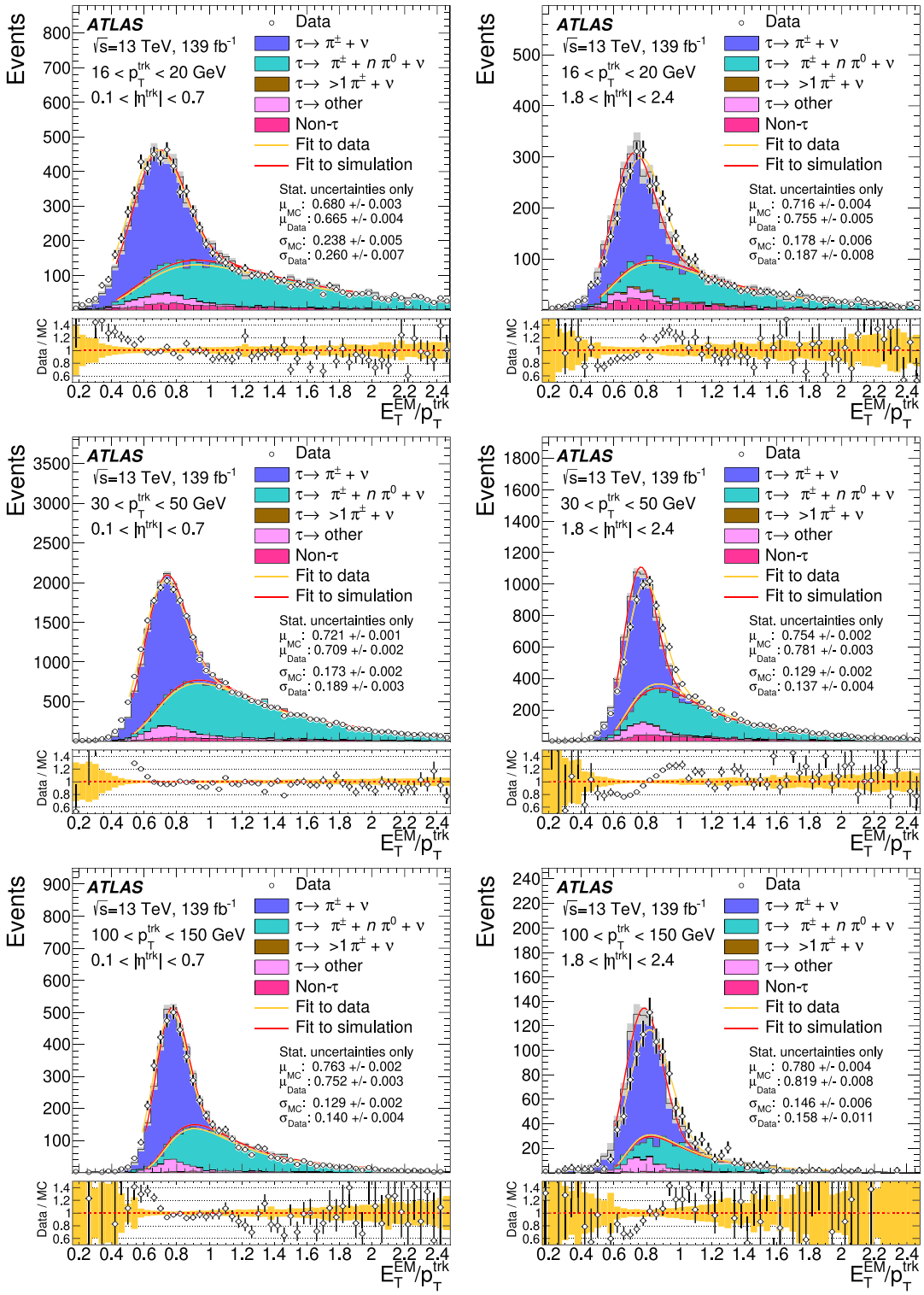

Fig. 1 Examples of the $E_{\mathrm{T}}^{\mathrm{EM}}/p_{\mathrm{T}}^{\mathrm{trk}}$ distribution and fit performed in the $16 < p_{\mathrm{T}}^{\mathrm{trk}} < 20$ GeV (top), $30 < p_{\mathrm{T}}^{\mathrm{trk}} < 50$ GeV (middle) and $100 < p_{\mathrm{T}}^{\mathrm{trk}} < 150$ GeV (bottom) bins in the barrel (left) and endcaps (right). The data are shown by points with a stacked histogram for simulation. The component where τ-leptons decay to multiple charged pions is small and difficult to see. The red fits correspond to simulation and the yellow fits correspond to data. Both the fits to the full distribution of a Gaussian+Landau function and just the Landau component from this fit are shown. The uncertainties shown are those from the statistics of the dataset and the limited Monte Carlo sample size. The bottom panel shows the ratio of data to simulation with statistical error bars on the data points and a yellow band illustrating the statistical uncertainty of the simulation. The simulation is normalised to the integral of the data

5 Calorimeter response measurement and comparison with simulation

The data are binned in both the track p_{T} and track $|\eta|$ to probe the calorimeter response at different momenta and in different regions. The calorimeter response is expected to vary significantly across $|\eta|$ due to the geometry and different calorimeter technologies. In the central region there is a large region which is expected to have a uniform response due to similar calorimeter structures up to $|\eta| = 0.7$. As the rejection of muons is more difficult at $|\eta| \sim 0$ a *barrel* selection region is defined by $0.1 < |\eta| < 0.7$. In this region there is a high-granularity liquid-argon/lead electromagnetic calorimeter and a steel/scintillator hadronic calorimeter. Another uniform detector region exists in the *endcap* region of $1.8 < |\eta| < 2.4$, where there is liquid-argon/lead electromagnetic calorimetry and liquid-argon/copper hadronic calorimetry. Due to differences in technology and material in the two regions, differences in the modelling might be expected. To study the response across the detector, results are shown for three $p_{\mathrm{T}}^{\mathrm{trk}}$ bins: $30 < p_{\mathrm{T}}^{\mathrm{trk}} < 50$ GeV, $50 < p_{\mathrm{T}}^{\mathrm{trk}} < 70$ GeV and $70 < p_{\mathrm{T}}^{\mathrm{trk}} < 100$ GeV, as a function of $|\eta^{\mathrm{trk}}|$.

Figure 2 shows the fitted response for the *barrel* and *endcap* regions defined above, as a function of the track p_{T}. Clear differences are seen between the data and simulation in both regions, with a ∼2% overestimate of the response in simulation in the barrel and a ∼4% underestimate of the response in simulation in the endcaps relative to the data. The data/MC differences also follow the same trends as seen in the jet response in these two regions [3]. It is checked that the fits give a reasonable χ^2 per degree of freedom and are stable when the fitting range and binning of the data are altered. These plots only show the uncertainties from the limited number of events in the samples, and systematic uncertainties are discussed in the next section. At the highest energies the steeply falling momentum spectrum and the increasing track resolution produces a bias in the measured track momentum compared to the true pion transverse momentum, $p_{\mathrm{T}}^{\mathrm{true}}$, resulting in the distribution flattening in both data and simulation. The biases in simulation from $\langle p_{\mathrm{T}}^{\mathrm{trk}}/p_{\mathrm{T}}^{\mathrm{true}}\rangle$ in the central (endcap) region for the highest three $p_{\mathrm{T}}^{\mathrm{trk}}$ bins are [0.2%, 0.8%, 1.7%] ([1.7%, 4.7%, 10.8%]).

Figure 3 shows the fitted response across the detector in fine $|\eta^{\mathrm{trk}}|$ bins for the three different $p_{\mathrm{T}}^{\mathrm{trk}}$ bins which have the most events. The calorimeter structure is clearly seen and the simulation follows the data, but some differences are present. The largest disagreements are ∼5% in the $1.0 < |\eta^{\mathrm{trk}}| < 1.2$ region. When the two sides of the detector are analysed independently the same trends are seen in the response. Additionally, when the analysis is performed separately for positively and negatively charged tracks consistent results are seen. In this energy regime the responses to π^+ and π^- are expected to be very similar and this check also tests the alignment of the inner detector as alignment errors would have different effects on positive and negative tracks.

6 Uncertainties in the response measurement

Several different effects could bias the measurements of the calorimeter response scale. These include uncertainties in the methodology of the fitting procedure, the backgrounds entering the event selection, the corrections for the effects of pile-up, and the modelling of tracks. The methods used to assess each of the different sources are described below and

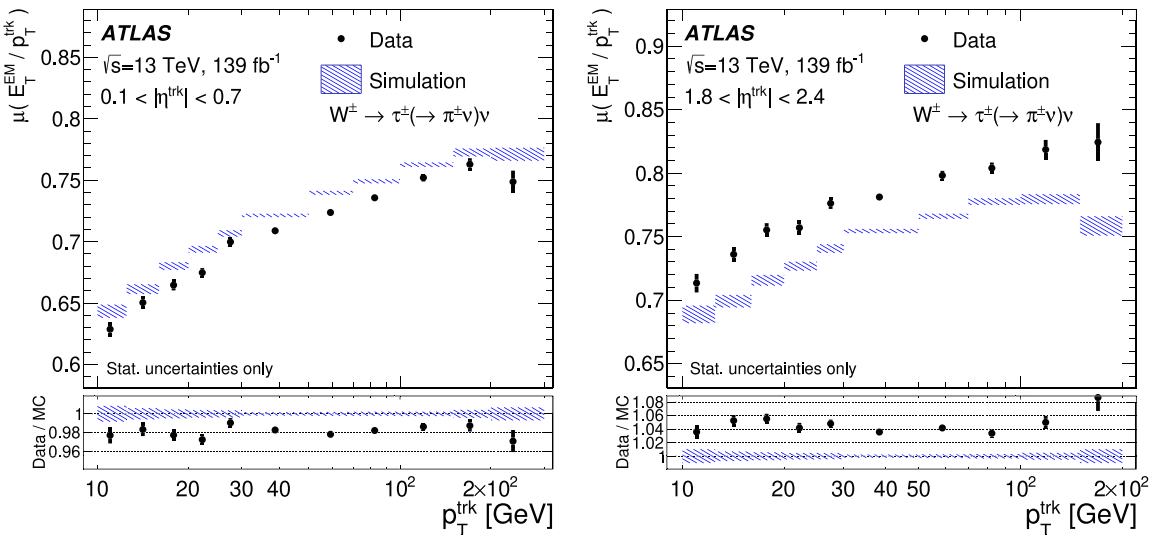

Fig. 2 The fitted mean of the signal $E_{\mathrm{T}}^{\mathrm{EM}}/p_{\mathrm{T}}^{\mathrm{trk}}$ distribution as a function of the track p_{T} in the central region (left) and endcap region (right). The error bars and uncertainty band show only the statistical uncertainties from the size of the dataset and simulated samples respectively

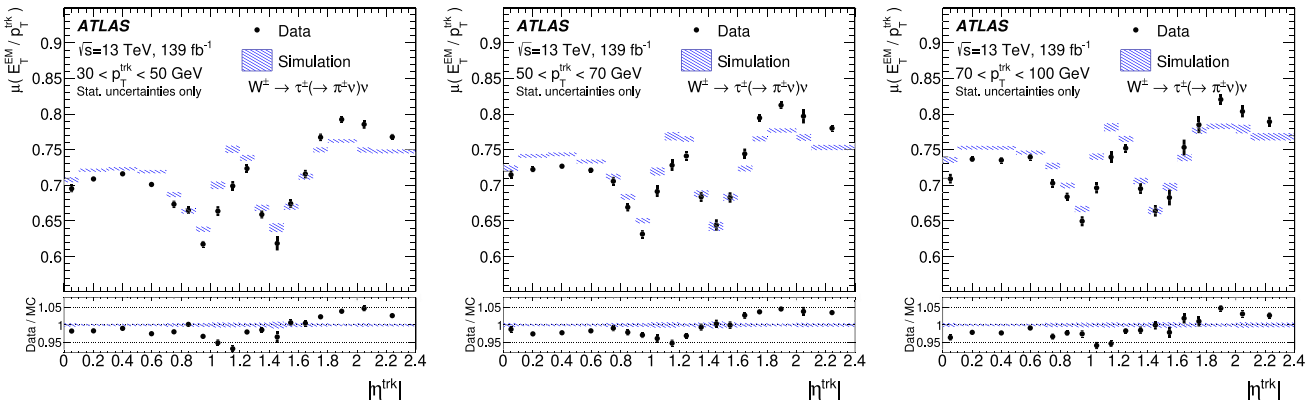

Fig. 3 The fitted mean of the signal $E_{\mathrm{T}}^{\mathrm{EM}}/p_{\mathrm{T}}^{\mathrm{trk}}$ distribution as a function of the track $|\eta^{\mathrm{trk}}|$ in three different $p_{\mathrm{T}}^{\mathrm{trk}}$ bins. The error bars and uncertainty band show only the statistical uncertainties from the size of the dataset and simulated samples respectively

are then summarised in Figs. 4 and 5. All uncertainties which are determined from a difference with respect to the nominal result are symmetrised.

Fit function (closure): A Gaussian+Landau fit to the signal and background is used to extract the calorimeter response scale. This is quantified in simulation by the difference between the fitted mean obtained from a Gaussian fit to just the signal $W^{\pm} \rightarrow \tau^{\pm}(\rightarrow \pi^{\pm}\nu_{\tau})\nu_{\tau}$ events and the fitted mean of the Gaussian function obtained from a combined Gaussian+Landau fit to the simulated signal and background. This closure test is seen to perform very well, showing that the Landau function choice is appropriate. The difference between the two values obtained is taken as a systematic uncertainty of the measurement. It is found to be subdominant and typically at the ∼0.2% level.

Bias in the fitted background shape: The shape of the background is taken from a fit to simulation, which could be biased relative to the shape in data. The background is primarily $W^{\pm} \rightarrow \tau^{\pm}(\rightarrow \pi^{\pm}n\pi^{0}\nu_{\tau})\nu_{\tau}$ events. Imperfections in the simulation of the shape of this background can come from detector effects such as the energy response to the charged and neutral pions, or from the energy spectra of the charged and neutral pions as modelled by the MC generator. The energy scale and resolution for electromagnetic showers, such as those from $\pi^0 \rightarrow \gamma\gamma$ decays, has been measured in ATLAS [74] and is known better than that for the hadronic showers probed here. The impact of detector mismodelling is tested by shifting or smearing the simulated response and evaluating the change in the fit when it is applied to data with the altered background shape. The hadronic response is shifted down (up) by 3% (5%) in the central (endcap) region, and separately smeared to increase the resolution by 10%. These values are determined from the discrepancies between data and simulation observed in this analysis. The smearing in the central region, and scale variation in the endcaps, produce significant uncertainties in the final results. To assess the modelling of the shape an alternative generator is used for the W+jets background; no significant impact on the shape is seen, so this is neglected. Therefore, the uncertainty in the shape of the fitted background is dominated by the detector modelling.

Electron and muon contamination: Contamination from electrons and muons is expected to be small: less than 0.4% and 0.7% respectively. The residual contamination is tested by tightening the criteria to reject these events: requiring the fraction of energy in the hadronic calorimeters to be >20%, and that there are no associated muon segments. Changes in the measured response in data define the uncertainty for muons. For electrons the difference between the changes in the measured response in data and simulation defines the uncertainty because the hadronic energy fraction cut can also bias the signal. Both of these uncertainties are found to be smaller than the statistical uncertainties of the measurement.

Non-lepton backgrounds: There is a small amount of background where the track does not originate from a lepton. The $Z(\rightarrow \nu\nu)$+jets contamination can be reduced by a tighter selection on the transverse mass of the track and the $E_{\mathrm{T}}^{\mathrm{miss}}$. The deviation from the nominal response when the upper bound on m_{T} is reduced by 10 GeV is taken as an uncertainty in this background. Additionally, the deviation from the nominal response when events with $m_{\mathrm{T}} < 10$ GeV are excluded is taken as an uncertainty in the potential contamination from events where the $E_{\mathrm{T}}^{\mathrm{miss}}$ comes from detector effects. These are also found to be smaller than the statistical uncertainties.

Pile-up uncertainties: Two uncertainties in the subtraction of the contributions from pile-up are considered. Nonlinearities in the required corrections can lead to imperfections in the removal of the effects of pile-up. The *closure* of the pile-up corrections is tested by taking half the difference between the responses for two large single-particle samples

with different pile-up, $\langle\mu^{\mathrm{PU}}\rangle \sim 20$ and $\langle\mu^{\mathrm{PU}}\rangle \sim 50$, after the corrections. Additionally, the *pile-up residual* correction is determined from simulation where pile-up might not be well modelled. Studies of the μ^{PU} dependence of the median p_{T} density of the event, ρ, the number of clusters, and the cell energy and noise find that the modelling of the energy flow in the simulation is within 10%–20% of the data across the detector. Therefore, 25% of the residual correction is taken as an uncertainty in the modelling of pile-up, which forms a minor uncertainty in the analysis. In data it is checked that the fitted response is stable with respect to pile-up by splitting the dataset into two independent datasets via high pile-up and low pile-up selections based on μ^{PU}, and also into three independent datasets, and no significant differences given the statistical uncertainties are seen in the measured response.

Tracking uncertainties: Any bias in the momentum scale of the reconstructed tracks directly affects the measurement. Muons are precisely calibrated using $Z \to \mu\mu$ and $J/\psi \to \mu\mu$ events. The analysis selection is modified by removing the m_{T} and transverse impact parameter requirements and requiring that a reconstructed muon is matched to the isolated track. The p_{T} of the track and muon are obviously correlated but fits to $p_{\mathrm{T}}^{\mathrm{trk}}/p_{\mathrm{T}}^{\mu}$ probe the inner-detector track scale relative to the calibrated muons. Two components are considered, the uncertainty in the calibration of muons and the statistical uncertainties of this cross-calibration, as none of the deviations of simulation from data are significant. Additionally, differences in the track resolution can bias the measurement because of the underlying falling $p_{\mathrm{T}}^{\mathrm{trk}}$ spectrum. The uncertainty in the momentum resolution of tracks is determined using the muons as described in Ref. [85]. Tracks are smeared to increase the resolution in simulation within the uncertainties and the impact on the parameter of interest is symmetrised and taken as an uncertainty.

The various systematic uncertainties are smoothed [86] across p_{T} as they are expected to vary smoothly. Across $|\eta|$, changes in the detector technology could result in sharp changes in the size of the systematic uncertainties. However, no such variations are seen, so the systematic uncertainties are also smoothed in the measurements as a function of $|\eta|$. The statistical components in data and simulation are not smoothed. The statistical uncertainty of the data is the largest uncertainty component in much of the phase space covered by the analysis.

Figure 4 shows the uncertainty from each source as a function of track p_{T} for the central and endcap regions. The uncertainty from imperfect knowledge of the background width (scale) in the central (endcap) region, and pile-up uncertainties in the endcap region, are the only uncertainties that are larger than the statistical uncertainty of the dataset or the simulated event samples in certain bins. The pile-up uncertainties have some importance at low p_{T}, and the tracking uncertainties grow at large track momentum. Overall, in the central region the total uncertainty is $\lesssim$1% for $20 < p_{\mathrm{T}} < 200$ GeV and reaches <0.6% in the most precise region. The test-beam uncertainties are about 2% in the barrel region [12], demonstrating the power of this in situ technique. In the endcaps the uncertainties are slightly larger but are $\lesssim$1% for $30 < p_{\mathrm{T}} < 100$ GeV. Figure 5 shows the uncertainties in the measurements as a function of $|\eta^{\mathrm{trk}}|$. The uncertainties are slightly larger due to the limited number of events in the smaller bins used to make fine calorimeter structures visible, but are otherwise dominated by the same sources as in the measurements as a function of p_{T}.

Having established the full uncertainties in the measurement, a calibration can be derived which can form an input to the high-p_{T} jet uncertainties [3] and also to the scale uncertainties for hadronic τ-lepton decays [19]. Figure 6 shows the measured data to simulation ratio of the response and its uncertainty in different $p_{\mathrm{T}}^{\mathrm{trk}}$ bins in the central and endcap regions. It is expected that such a calibration will be smooth across p_{T}. The same procedure as used for the jet energy scale is used [3,87] to translate the binned measurements and uncertainties into smooth uncertainty eigenvectors and a smooth calibration curve. Each of the measurements is divided into finer bins of 0.1 GeV using second-order polynomial splines. The final calibration curve is determined by smoothing the measurements with a Gaussian kernel of varying width. Each individual uncertainty component is treated as correlated across p_{T} and is then propagated through the same procedure after varying it by 1σ. The difference between the calibration curve with the shifted systematic uncertainty input and the nominal calibration curve is taken as 1σ in the varied uncertainty. Each uncertainty source is treated as correlated across p_{T} and uncorrelated with all other sources of uncertainty. This smoothing procedure reduces statistical fluctuations in the central values and in each propagated uncertainty component. Therefore, the final uncertainties are slightly smaller than those for the corresponding individual measurement points. The resulting smooth calibration curve and uncertainty band are shown in Fig. 6.

Figure 7 shows the data/MC ratio as a function of $|\eta^{\mathrm{trk}}|$ for the three measured p_{T} ranges along with the associated uncertainties. As the changes in detector technology can result in sharp features in the calibration as a function of $|\eta^{\mathrm{trk}}|$ a smooth calibration curve is not derived for these results.

7 Width of the $E_{\mathrm{T}}^{\mathrm{EM}}/p_{\mathrm{T}}^{\mathrm{trk}}$ distribution

The width of the $E_{\mathrm{T}}^{\mathrm{EM}}/p_{\mathrm{T}}^{\mathrm{trk}}$ distribution probes the resolution of both the tracker and the calorimeter; however, the tracking component is relatively small outside of the highest energy bins. The width will also contain components

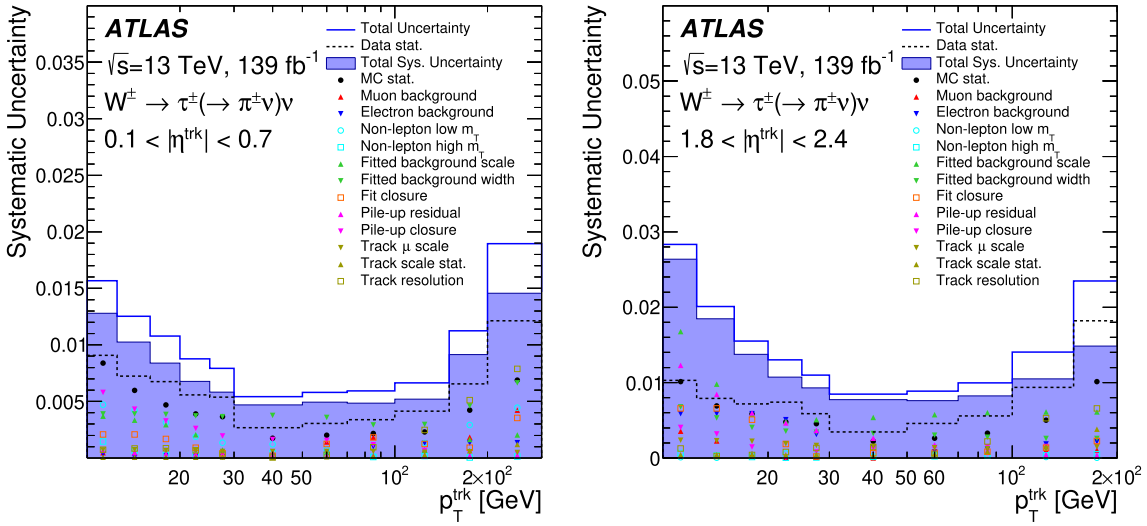

Fig. 4 The various systematic uncertainties which affect the measurement of the calorimeter energy scale for charged pions as a function of $p_{\mathrm{T}}^{\mathrm{trk}}$ in the central (left) and endcap (right) regions

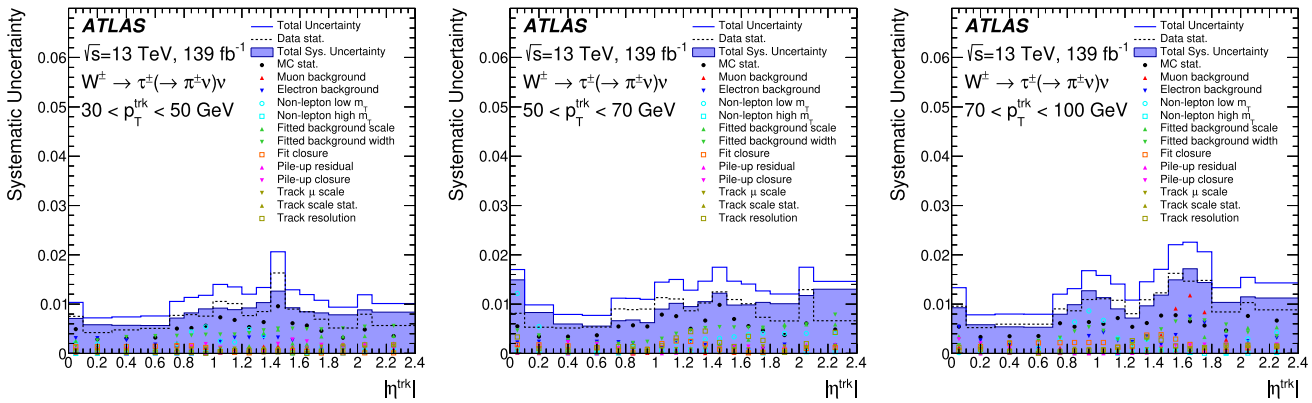

Fig. 5 The various systematic uncertainties which affect the measurement of the calorimeter energy scale for charged pions as a function of $|\eta^{\mathrm{trk}}|$ for three $p_{\mathrm{T}}^{\mathrm{trk}}$ ranges: $30 < p_{\mathrm{T}}^{\mathrm{trk}} < 50$ GeV, $50 < p_{\mathrm{T}}^{\mathrm{trk}} < 70$ GeV and $70 < p_{\mathrm{T}}^{\mathrm{trk}} < 100$ GeV

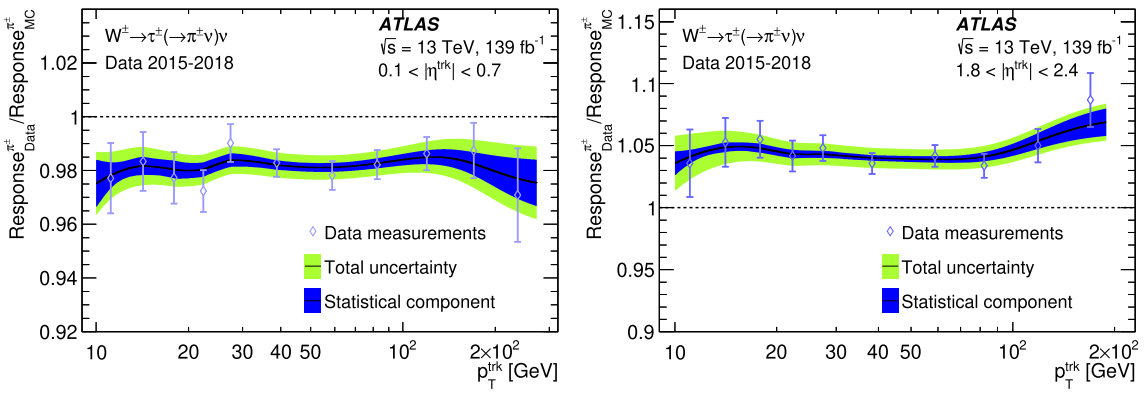

Fig. 6 The measured data to simulation ratio of the response as a function of $p_{\mathrm{T}}^{\mathrm{trk}}$ for the barrel (left) and endcaps (right). Points represent the different measurement bins with their total uncertainty from both the statistical and systematic sources. Also shown is the smooth calibration curve with its associated uncertainties

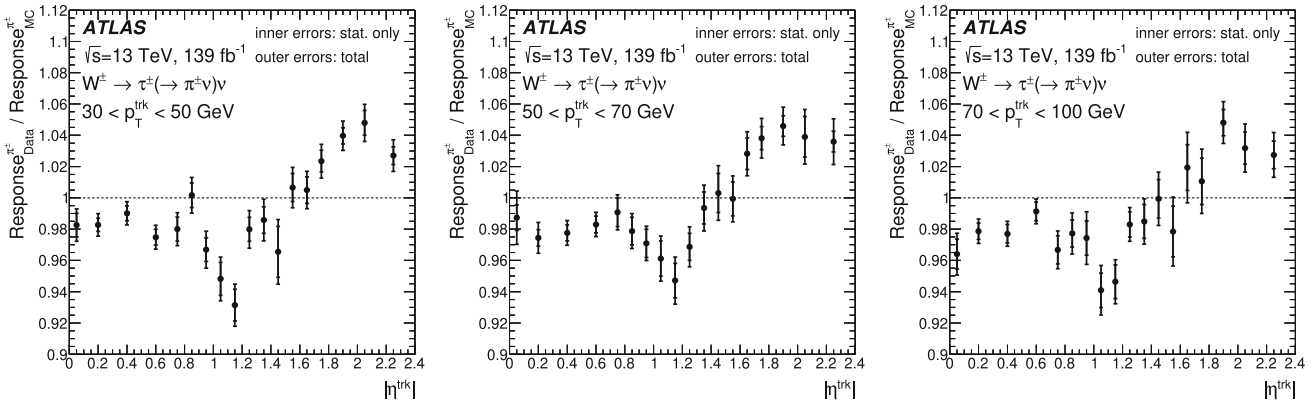

Fig. 7 The measured data to simulation ratio of the response as a function of $|\eta^{\text{trk}}|$ for the three $p_{\text{T}}^{\text{trk}}$ ranges: $30 < p_{\text{T}}^{\text{trk}} < 50$ GeV, $50 < p_{\text{T}}^{\text{trk}} < 70$ GeV and $70 < p_{\text{T}}^{\text{trk}} < 100$ GeV. Inner error bars represent uncertainties from limited sample size and the outer error bars give the total uncertainty including both the statistical errors and systematic uncertainties

from the modelling of pile-up noise falling into the region of the calorimeter considered in the measurement. These can be reliably corrected for in measurements of the scale, but the effect on the resolution is much harder to mitigate, so the level of agreement between simulation and data, which both include these effects, is considered. The increase in the width of $E_{\text{T}}^{\text{EM}}/p_{\text{T}}^{\text{trk}}$ due to the effects of pile-up is measured by looking at the difference between the width in two simulated samples with $\langle\mu^{\text{PU}}\rangle \sim 20$ and $\langle\mu^{\text{PU}}\rangle \sim 50$. For the central (endcap) region the difference is found to be 8% (16%) for $16 < p_{\text{T}}^{\text{trk}} < 20$ GeV and 3% (12%) for $30 < p_{\text{T}}^{\text{trk}} < 150$ GeV. The impact of mismodelling the pile-up is expected to be small for most of the $p_{\text{T}}^{\text{trk}}$ spectrum since the simulation includes pile-up and should capture most of the effect. Figure 8 shows the relative width of the $E_{\text{T}}^{\text{EM}}/p_{\text{T}}^{\text{trk}}$ distribution as a function of track p_{T} in the central and endcap regions. In the central region the simulation shows about 10% better resolution than the data, while in the endcaps the level of agreement is generally better. The relative width across $|\eta|$ is shown for three $p_{\text{T}}^{\text{trk}}$ bins in Fig. 9. In both figures the resolution for tracks selected in simulation is found to contribute significantly at high momentum, but across much of the spectrum it is significantly smaller than the calorimeter contributions, indicating that the discrepancies between simulation and data are more likely due to the simulation of the calorimeter response.

In the central region where the statistical uncertainties are lower, $30 < p_{\text{T}}^{\text{trk}} < 150$ GeV, it is possible to check if any of the systematic effects considered in Sect. 6 could be the source of the discrepancies. The closure of the fits to obtain the width of the signal component is very good, with differences only at the level of $\lesssim$2% at $p_{\text{T}}^{\text{trk}}$ of 30 GeV and $\lesssim$1% above 50 GeV. Tightening the selections to reject electrons and muons has a minimal effect on the measured resolution, $\lesssim$0.5%. Shifting the response scale of the background and smearing the background response are each seen to change the resolution in data by $\lesssim$1% in this region of phase space. Tightening the criteria to reject non-lepton backgrounds also results in small changes of $\lesssim$0.5% beyond 30 GeV. Therefore, resolution discrepancies of $\sim$10% between data and simulation are significant in this $p_{\text{T}}^{\text{trk}}$ range compared to the potential systematic effects on the extraction of the $E_{\text{T}}^{\text{EM}}/p_{\text{T}}^{\text{trk}}$ width. Below 30 GeV the fit closure grows to up to 6% and the uncertainties related to the fitted background shape and the non-lepton backgrounds all increase to $\lesssim$1.5%, so that at low momentum the discrepancies are less significant.

This supports the observation in the jet resolution measurement using p_{T} balance in dijet events that the resolution in simulation is slightly superior to that in data [3] at medium to high p_{T} and this is therefore an area where it is desirable to improve the simulation.

8 Measurements of the longitudinal energy profile and late showering particles

The longitudinal segmentation of the calorimeter into layers can be used to gain insight into the cause of the discrepancies in the scale and resolution between data and simulation. Backgrounds can bias any measurements of average energies deposited in a single layer. In the electromagnetic calorimeter the main background, $\tau^{\pm} \to \pi^{\pm} + n\pi^0 + \nu_{\tau}$, will result in significant biases as the $\pi^0 \to \gamma\gamma$ showers will be contained within the electromagnetic calorimeter. Therefore, only the energy deposited in the hadronic calorimeter layers is considered, although these measurements are still slightly biased by this background through selection effects because the events are required to pass the hadronic energy fraction requirement. The hadronic calorimeter is less affected by pile-up since low-momentum hadrons are often contained within the

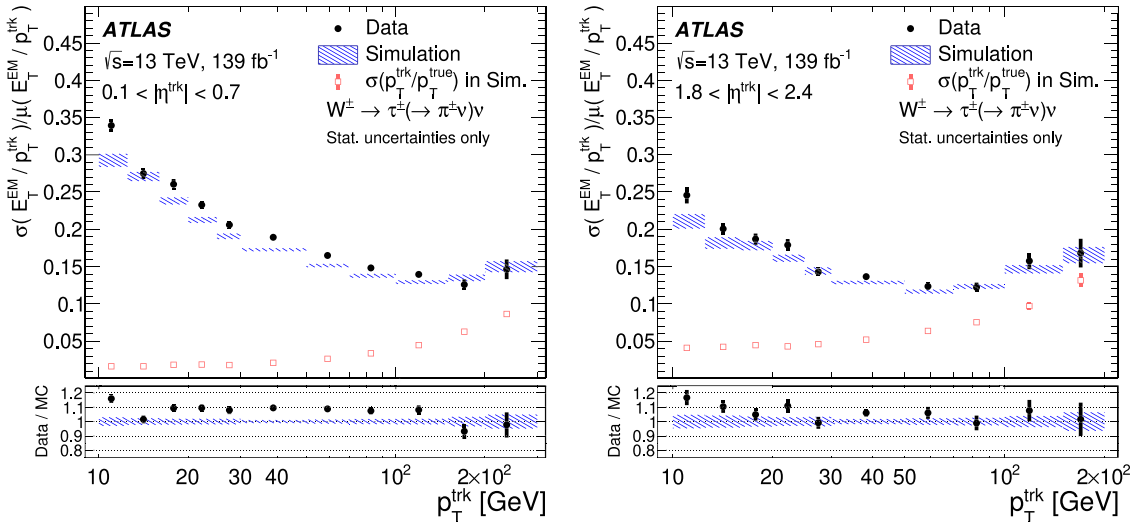

Fig. 8 The fitted width divided by the mean of the signal $E_{\mathrm{T}}^{\mathrm{EM}}/p_{\mathrm{T}}^{\mathrm{trk}}$ distribution as a function of the track p_{T} in the central region (left) and endcap region (right). Also shown is the fitted width of the track p_{T} divided by the generator-level p_{T} for true $\tau \to \pi^{\pm}\nu_{\tau}$ events in simulation to give an illustration of the contribution to the total width from the resolution of reconstructed tracks. The uncertainties shown are only those from the limited number of events in the dataset and simulated samples

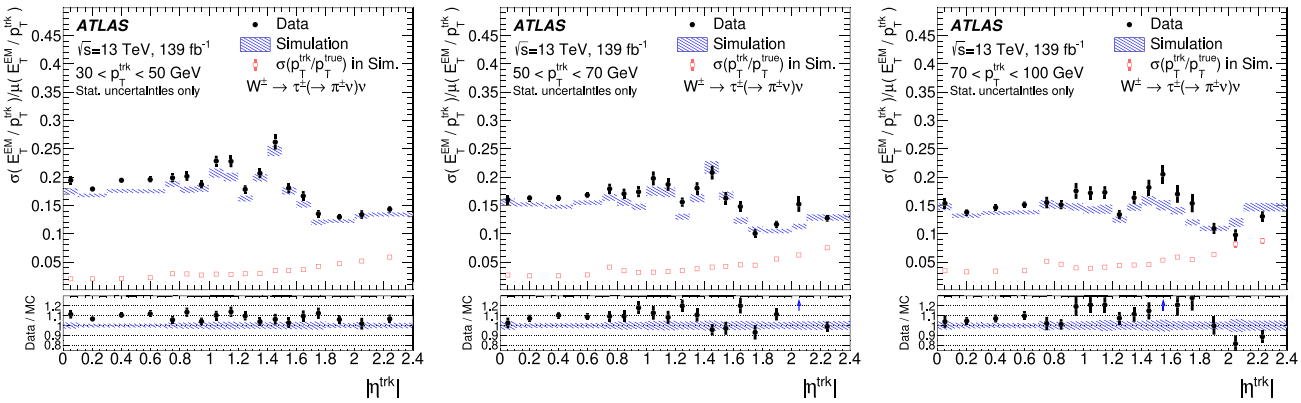

Fig. 9 The fitted width divided by the mean of the signal $E_{\mathrm{T}}^{\mathrm{EM}}/p_{\mathrm{T}}^{\mathrm{trk}}$ distribution as a function of the track $|\eta|$ in three $p_{\mathrm{T}}^{\mathrm{trk}}$ ranges: $30 < p_{\mathrm{T}}^{\mathrm{trk}} < 50$ GeV, $50 < p_{\mathrm{T}}^{\mathrm{trk}} < 70$ GeV and $70 < p_{\mathrm{T}}^{\mathrm{trk}} < 100$ GeV. Also shown is the fitted width of the track p_{T} divided by the generator-level p_{T} for true $\tau \to \pi^{\pm}\nu_{\tau}$ events in simulation to give an illustration of the contribution to the total width from the resolution of reconstructed tracks. The uncertainties shown are only those from the limited number of events in the dataset and simulated samples

electromagnetic calorimeter in addition to the pile-up particles that produce electromagnetic showers.

Figure 10 shows the average energy deposited in each layer of the hadronic calorimeter divided by the track momentum in the barrel and endcap regions as a function of the track p_{T}. Events are required to have $0.2 < E_{\mathrm{T}}^{\mathrm{EM}}/p_{\mathrm{T}}^{\mathrm{trk}} < 1.1$ to select events across the full response and also minimise the contribution from backgrounds. An arithmetic mean of all the selected events is used because the distribution of the energy in an individual layer is not expected to have a Gaussian shape. It can be seen that in the barrel the simulation overestimates the relative energy in the hadronic calorimeter by 3-5% across the p_{T} spectrum and this is the case in all layers, although most of the energy is contained within the first two layers. In the endcap region the amount of energy in the hadronic layers is slightly underestimated overall. This is driven by an underestimation of the energy in the first layer. Both of these features are in line with the results in Sect. 5; however, the magnitude of the difference in the energy deposited does not explain the size of the effect seen in the total response, indicating that there is mismodelling either in both the electromagnetic and hadronic calorimeters or in the length of the shower, or in a combination of these or other effects. The results are seen to be largely unaffected by pile-up. These results can be used for the tuning of the detector simulation.

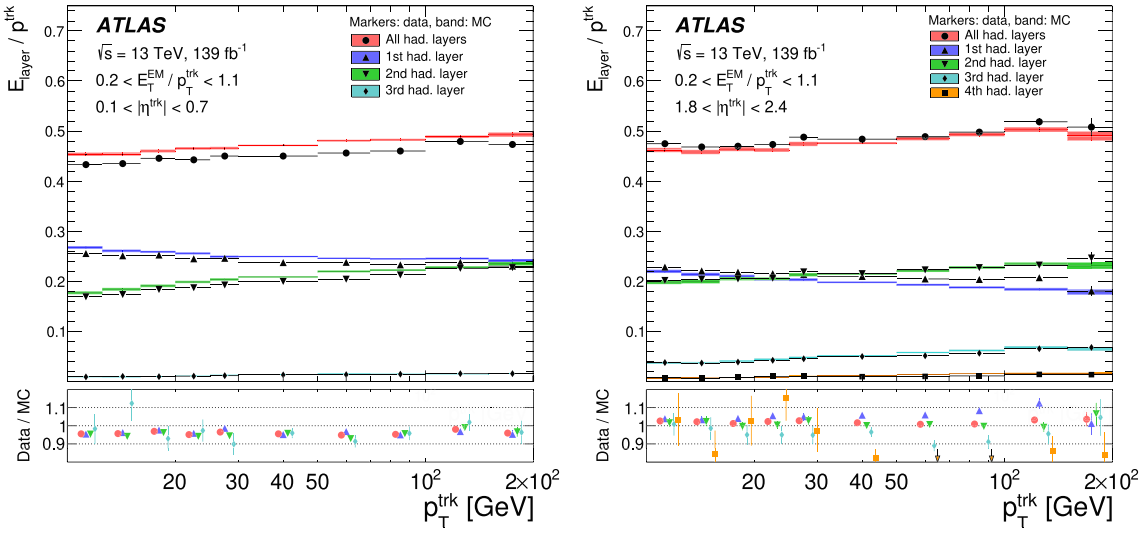

Fig. 10 The average energy within each hadronic layer normalised to the track momentum as a function of track p_{T} in the barrel (left) and endcaps (right). Also shown are the ratios of the sum of energies in all layers of the hadronic calorimeter to the track momentum. Data are required to have $0.2 < E_{\mathrm{T}}^{\mathrm{EM}}/p_{\mathrm{T}}^{\mathrm{trk}} < 1.1$ to primarily select single-pion events. Shown in the lower panel is the ratio of data to simulation. The error bars and uncertainty band show the uncertainties from the limited number of events in the dataset and simulated samples

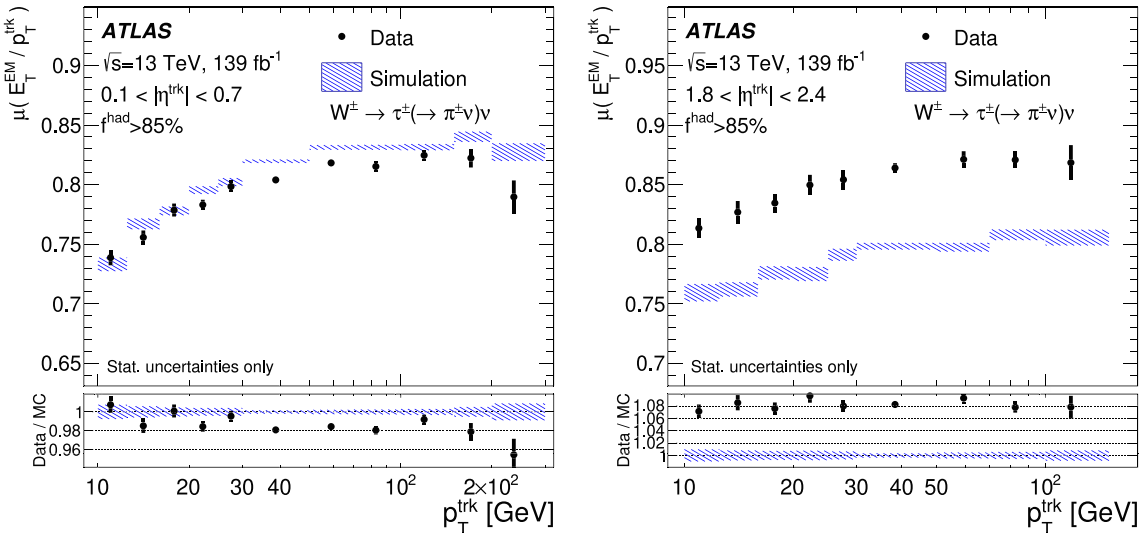

Fig. 11 The fitted response as a function of track p_{T} in the barrel (left) and endcaps (right) after requiring the fraction of the associated energy that is in the hadronic calorimeters to satisfy $f^{\mathrm{had}} > 85\%$. The error bars and uncertainty band show the uncertainties from the limited number of events in the dataset and simulated samples respectively

A second method of using the longitudinal segmentation to probe the sources of the discrepancies is to select events where the pion traverses the electromagnetic calorimeter as a minimally ionising particle before showering in the hadronic calorimeter layers. Such events are characterised by having a very large fraction of their energy in the hadronic calorimeter. Selecting events in which more than 85% of the summed cluster energy is in the hadronic calorimeters, $f^{\mathrm{had}} > 85\%$, allows the data-to-MC response ratio to be probed in the hadronic calorimeters. Figure 11 shows the fitted response after applying this selection criterion in the barrel and endcap regions. In the barrel region the data-to-MC response ratio is seen to be similar to the inclusive response ratio; however, larger discrepancies are seen in the endcaps after this selection, with the difference between data and simulation increasing from ∼4% to ∼8%. This suggests that the simulation models hadronic showers in the hadronic calorimeter less accurately in the endcaps than in the inclusive case.

9 Conclusion

The energy response of the ATLAS calorimeter has been measured across a wide range of pion momenta with high precision using an innovative technique based on isolated charged pions from the process $W^{\pm} \to \tau^{\pm}(\to \pi^{\pm} + \nu_{\tau})\nu_{\tau}$. The calorimeter response is observed to be overestimated by ∼2% in the central region and underestimated by ∼4% in the endcaps in the ATLAS simulation. This supports the observations in the measurement of the jet energy scale, which show a similar structure across the calorimeter [3]. The precision of the measurement of the response is $\lesssim$1% for $15 < p_{\mathrm{T}} < 185$ GeV ($20 < p_{\mathrm{T}} < 100$ GeV) in the central (endcap) regions, and is <0.6% in the most precise region, $20 < p_{\mathrm{T}} < 120$ GeV in the barrel.

The width of the $E_{\mathrm{T}}^{\mathrm{EM}}/p_{\mathrm{T}}^{\mathrm{trk}}$ distribution has also been investigated. This measurement convolves the tracking and calorimeter resolutions. For this quantity the simulation is found to agree with the data to within 15%; however, the data are generally observed to have a wider distribution. Finally, the average energy in the layers of the hadronic calorimeter was probed as a method of investigating the cause of the discrepancies between the simulation and the data. These measurements will be used in the tuning of the ATLAS simulation to further improve the hadron shower modelling and detector geometry.

This powerful new method of measuring the hadronic energy response of the ATLAS calorimeter can achieve a precision of $\lesssim$1% for the response of the calorimeter to charged pions. This detailed understanding of the response of the calorimeter can be used in gaining better understanding of the jet energy scale, its uncertainty for the highest-p_{T} jets, the energy scale of hadronically decaying τ-leptons, and in measuring the properties of jets.

Acknowledgements We thank CERN for the very successful operation of the LHC, as well as the support staff from our institutions without whom ATLAS could not be operated efficiently. We acknowledge the support of ANPCyT, Argentina; YerPhI, Armenia; ARC, Australia; BMWFW and FWF, Austria; ANAS, Azerbaijan; SSTC, Belarus; CNPq and FAPESP, Brazil; NSERC, NRC and CFI, Canada; CERN; ANID, Chile; CAS, MOST and NSFC, China; Minciencias, Colombia; MSMT CR, MPO CR and VSC CR, Czech Republic; DNRF and DNSRC, Denmark; IN2P3-CNRS and CEA-DRF/IRFU, France; SRNSFG, Georgia; BMBF, HGF and MPG, Germany; GSRI, Greece; RGC and Hong Kong SAR, China; ISF and Benoziyo Center, Israel; INFN, Italy; MEXT and JSPS, Japan; CNRST, Morocco; NWO, Netherlands; RCN, Norway; MEiN, Poland; FCT, Portugal; MNE/IFA, Romania; JINR; MES of Russia and NRC KI, Russian Federation; MESTD, Serbia; MSSR, Slovakia; ARRS and MIZŠ, Slovenia; DSI/NRF, South Africa; MICINN, Spain; SRC and Wallenberg Foundation, Sweden; SERI, SNSF and Cantons of Bern and Geneva, Switzerland; MOST, Taiwan; TAEK, Turkey; STFC, United Kingdom; DOE and NSF, United States of America. In addition, individual groups and members have received support from BCKDF, CANARIE, Compute Canada and CRC, Canada; COST, ERC, ERDF, Horizon 2020 and Marie Skłodowska-Curie Actions, European Union; Investissements d'Avenir Labex, Investissements d'Avenir Idex and ANR, France; DFG and AvH Foundation, Germany; Herakleitos, Thales and Aristeia programmes co-financed by EU-ESF and the Greek NSRF, Greece; BSF-NSF and GIF, Israel; Norwegian Financial Mechanism 2014-2021, Norway; NCN and NAWA, Poland; La Caixa Banking Foundation, CERCA Programme Generalitat de Catalunya and PROMETEO and GenT Programmes Generalitat Valenciana, Spain; Göran Gustafssons Stiftelse, Sweden; The Royal Society and Leverhulme Trust, United Kingdom. The crucial computing support from all WLCG partners is acknowledged gratefully, in particular from CERN, the ATLAS Tier-1 facilities at TRIUMF (Canada), NDGF (Denmark, Norway, Sweden), CC-IN2P3 (France), KIT/GridKA (Germany), INFN-CNAF (Italy), NL-T1 (Netherlands), PIC (Spain), ASGC (Taiwan), RAL (UK) and BNL (USA), the Tier-2 facilities worldwide and large non-WLCG resource providers. Major contributors of computing resources are listed in Ref. [88].

Data Availability Statement This manuscript has no associated data or the data will not be deposited. [Authors' comment: All ATLAS scientific output is published in journals, and preliminary results are made available in Conference Notes. All are openly available, without restriction on use by external parties beyond copyright law and the standard conditions agreed by CERN. Data associated with journal publications are also made available: tables and data from plots (e.g. cross section values, likelihood profiles, selection efficiencies, cross section limits, ...) are stored in appropriate repositories such as HEPDATA (http://hepdata.cedar.ac.uk/). ATLAS also strives to make additional material related to the paper available that allows a reinterpretation of the data in the context of new theoretical models. For example, an extended encapsulation of the analysis is often provided for measurements in the framework of RIVET (http://rivet.hepforge.org/).]

Open Access This article is licensed under a Creative Commons Attribution 4.0 International License, which permits use, sharing, adaptation, distribution and reproduction in any medium or format, as long as you give appropriate credit to the original author(s) and the source, provide a link to the Creative Commons licence, and indicate if changes were made. The images or other third party material in this article are included in the article's Creative Commons licence, unless indicated otherwise in a credit line to the material. If material is not included in the article's Creative Commons licence and your intended use is not permitted by statutory regulation or exceeds the permitted use, you will need to obtain permission directly from the copyright holder. To view a copy of this licence, visit http://creativecommons.org/licenses/by/4.0/.
Funded by SCOAP[3].

References

1. ATLAS Collaboration, The ATLAS experiment at the CERN large hadron collider. JINST **3**, S08003 (2008). https://doi.org/10.1088/1748-0221/3/08/S08003
2. ATLAS Collaboration, Jet reconstruction and performance using particle flow with the ATLAS detector. Eur. Phys. J. C **77**, 466 (2017). https://doi.org/10.1140/epjc/s10052-017-5031-2. arXiv:1703.10485 [hep-ex]
3. ATLAS Collaboration, Jet energy scale and resolution measured in proton–proton collisions at $\sqrt{s} = 13$ TeV with the ATLAS detector. Eur. Phys. J. C **81**, 689 (2020). https://doi.org/10.1140/epjc/s10052-021-09402-3. arXiv:2007.02645 [hep-ex]
4. ATLAS Collaboration, Alignment of the ATLAS inner detector in Run 2. Eur. Phys. J. C **80**, 1194 (2020). https://doi.org/10.1140/epjc/s10052-020-08700-6. arXiv:2007.07624 [hep-ex]
5. ATLAS Collaboration, A measurement of the calorimeter response to single hadrons and determination of the jet energy scale uncer-

tainty using LHC Run-1 pp-collision data with the ATLAS detector. Eur. Phys. J. C **77**, 26 (2017). https://doi.org/10.1140/epjc/s10052-016-4580-0. arXiv:1607.08842 [hep-ex]
6. ATLAS Collaboration, Single hadron response measurement and calorimeter jet energy scale uncertainty with the ATLAS detector at the LHC. Eur. Phys. J. C **73**, 2305 (2013). https://doi.org/10.1140/epjc/s10052-013-2305-1. arXiv:1203.1302 [hep-ex]
7. ATLAS Collaboration, Electron and photon energy calibration with the ATLAS detector using 2015–2016 LHC proton–proton collision data. JINST **14**, P03017 (2019). https://doi.org/10.1088/1748-0221/14/03/P03017. arXiv:1812.03848 [hep-ex]
8. D.M. Gingrich et al., Performance of a large scale prototype of the ATLAS accordion electromagnetic calorimeter. Nucl. Instrum. Methods A **364**, 290 (1995). https://doi.org/10.1016/0168-9002(95)00406-8
9. D.M. Gingrich et al., Performance of an endcap prototype of the ATLAS accordion electromagnetic calorimeter. Nucl. Instrum. Methods A **389**, 398 (1997). https://doi.org/10.1016/S0168-9002(97)00328-8
10. P. Adragna et al., Testbeam studies of production modules of the ATLAS Tile calorimeter. Nucl. Instrum. Methods A **606**, 362 (2009). https://doi.org/10.1016/j.nima.2009.04.009
11. B. Dowler et al., Performance of the ATLAS hadronic end-cap calorimeter in beam tests. Nucl. Instrum. Methods A **482**, 94 (2002). https://doi.org/10.1016/S0168-9002(01)01338-9
12. E. Abat et al., Study of energy response and resolution of the ATLAS barrel calorimeter to hadrons of energies from 20 to 350 GeV. Nucl. Instrum. Methods A **621**, 134 (2010). https://doi.org/10.1016/j.nima.2010.04.054
13. ATLAS Collaboration, Study of the material of the ATLAS inner detector for Run 2 of the LHC. JINST **12**, P12009 (2017). https://doi.org/10.1088/1748-0221/12/12/P12009. arXiv:1707.02826 [hep-ex]
14. A. Ribon et al., Status of Geant4 hadronic physics for the simulation of LHC experiments at the start of LHC physics program. CERN-LCGAPP **2** (2010)
15. ATLAS Collaboration, Measurement of inclusive jet and dijet cross-sections in proton–proton collisions at $\sqrt{s} = 13$ TeV with the ATLAS detector. JHEP **05**, 195 (2018). https://doi.org/10.1007/JHEP05(2018)195. arXiv:1711.02692 [hep-ex]
16. ATLAS Collaboration, Evidence for $t\bar{t}t\bar{t}$ production in the multilepton final state in proton–proton collisions at $\sqrt{s} = 13$ TeV with the ATLAS detector. Eur. Phys. J. C **80**, 1085 (2020). https://doi.org/10.1140/epjc/s10052-020-08509-3. arXiv:2007.14858 [hep-ex]
17. ATLAS Collaboration, Search for new phenomena in events with an energetic jet and missing transverse momentum in pp collisions at $\sqrt{s} = 13$ TeV with the ATLAS detector. Phys. Rev. D **103**, 112006 (2021). https://doi.org/10.1103/PhysRevD.103.112006. arXiv:2102.10874 [hep-ex]
18. ATLAS Collaboration, Search for squarks and gluinos in final states with jets and missing transverse momentum using 139 fb^{-1} of $\sqrt{s} = 13$ TeV pp collision data with the ATLAS detector. JHEP **02**, 143 (2021). https://doi.org/10.1007/JHEP02(2021)143. arXiv:2010.14293 [hep-ex]
19. ATLAS Collaboration, Identification and energy calibration of hadronically decaying tau leptons with the ATLAS experiment in pp collisions at $\sqrt{s} = 8$ TeV. Eur. Phys. J. C **75**, 303 (2015). https://doi.org/10.1140/epjc/s10052-015-3500-z. arXiv:1412.7086 [hep-ex]
20. ATLAS Collaboration, Measurement of the soft-drop jet mass in pp collisions at $\sqrt{s} = 13$ TeV with the ATLAS detector. Phys. Rev. Lett. **121**, 092001 (2018). https://doi.org/10.1103/PhysRevLett.121.092001. arXiv:1711.08341 [hep-ex]
21. ATLAS Collaboration, Performance of top-quark and W-boson tagging with ATLAS in Run 2 of the LHC. Eur. Phys. J. C **79**, 375 (2019). https://doi.org/10.1140/epjc/s10052-019-6847-8. arXiv:1808.07858 [hep-ex]
22. ATLAS Collaboration, ATLAS insertable B-layer: technical design report. ATLAS-TDR-19; CERN-LHCC-2010-013 (2010). https://cds.cern.ch/record/1291633 [Addendum: ATLAS-TDR-19-ADD-1; CERN-LHCC-2012-009 (2012). https://cds.cern.ch/record/1451888]
23. B. Abbott et al., Production and integration of the ATLAS insertable B-layer. JINST **13**, T05008 (2018). https://doi.org/10.1088/1748-0221/13/05/T05008 arXiv:1803.00844 [physics.ins-det]
24. ATLAS Collaboration, Operation of the ATLAS trigger system in Run 2. JINST **15**, P10004 (2020). https://doi.org/10.1088/1748-0221/15/10/P10004. arXiv:2007.12539 [hep-ex]
25. ATLAS Collaboration, The ATLAS Collaboration software and firmware. ATL-SOFT-PUB-2021-001 (2021). https://cds.cern.ch/record/2767187
26. ATLAS Collaboration, Luminosity determination in pp collisions at $\sqrt{s} = 13$ TeV using the ATLAS detector at the LHC. ATLAS-CONF-2019-021 (2019). https://cds.cern.ch/record/2677054
27. ATLAS Collaboration, Performance of the missing transverse momentum triggers for the ATLAS detector during Run-2 data taking. JHEP **08**, 080 (2020). https://doi.org/10.1007/JHEP08(2020)080. arXiv:2005.09554 [hep-ex]
28. ATLAS Collaboration, ATLAS data quality operations and performance for 2015–2018 data-taking. JINST **15**, P04003 (2020). https://doi.org/10.1088/1748-0221/15/04/P04003. arXiv:1911.04632 [physics.ins-det]
29. G. Avoni et al., The new LUCID-2 detector for luminosity measurement and monitoring in ATLAS. JINST **13**, P07017 (2018). https://doi.org/10.1088/1748-0221/13/07/P07017
30. T. Gleisberg et al., Event generation with SHERPA 1.1. JHEP **02**, 007 (2009). https://doi.org/10.1088/1126-6708/2009/02/007 arXiv:0811.4622 [hep-ph]
31. E. Bothmann et al., Event generation with Sherpa 2.2. SciPost Phys. **7**, 034 (2019). https://doi.org/10.21468/SciPostPhys.7.3.034 arXiv:1905.09127 [hep-ph]
32. T. Gleisberg, S. Höche, Comix, a new matrix element generator. JHEP **12**, 039 (2008). https://doi.org/10.1088/1126-6708/2008/12/039 arXiv:0808.3674 [hep-ph]
33. F. Cascioli, P. Maierhöfer, S. Pozzorini, Scattering amplitudes with open loops. Phys. Rev. Lett. **108**, 111601 (2012). https://doi.org/10.1103/PhysRevLett.108.111601 arXiv:1111.5206 [hep-ph]
34. A. Denner, S. Dittmaier, L. Hofer, Collier: a Fortran-based complex one-loop library in extended regularizations. Comput. Phys. Commun. **212**, 220 (2017). https://doi.org/10.1016/j.cpc.2016.10.013 arXiv:1604.06792 [hep-ph]
35. S. Schumann, F. Krauss, A parton shower algorithm based on Catani–Seymour dipole factorisation. JHEP **03**, 038 (2008). https://doi.org/10.1088/1126-6708/2008/03/038 arXiv:0709.1027 [hep-ph]
36. S. Höche, F. Krauss, M. Schönherr, F. Siegert, A critical appraisal of NLO+PS matching methods. JHEP **09**, 049 (2012). https://doi.org/10.1007/JHEP09(2012)049 arXiv:1111.1220 [hep-ph]
37. S. Höche, F. Krauss, M. Schönherr, F. Siegert, QCD matrix elements + parton showers. The NLO case. JHEP **04**, 027 (2013). https://doi.org/10.1007/JHEP04(2013)027 arXiv:1207.5030 [hep-ph]
38. S. Catani, F. Krauss, B.R. Webber, R. Kuhn, QCD matrix elements + parton showers. JHEP **11**, 063 (2001). https://doi.org/10.1088/1126-6708/2001/11/063 arXiv:hep-ph/0109231
39. S. Höche, F. Krauss, S. Schumann, F. Siegert, QCD matrix elements and truncated showers. JHEP **05**, 053 (2009). https://doi.org/10.1088/1126-6708/2009/05/053 arXiv:0903.1219 [hep-ph]

40. R.D. Ball et al., Parton distributions for the LHC run II. JHEP **04**, 040 (2015). https://doi.org/10.1007/JHEP04(2015)040 arXiv:1410.8849 [hep-ph]
41. C. Anastasiou, L.J. Dixon, K. Melnikov, F. Petriello, High precision QCD at hadron colliders: electroweak gauge boson rapidity distributions at next-to-next-to leading order. Phys. Rev. D **69**, 094008 (2004). https://doi.org/10.1103/PhysRevD.69.094008 arXiv:hep-ph/0312266
42. S. Frixione, P. Nason, G. Ridolfi, A positive-weight next-to-leading-order Monte Carlo for heavy flavour hadroproduction. JHEP **09**, 126 (2007). https://doi.org/10.1088/1126-6708/2007/09/126 arXiv:0707.3088 [hep-ph]
43. P. Nason, A new method for combining NLO QCD with shower Monte Carlo algorithms. JHEP **11**, 040 (2004). https://doi.org/10.1088/1126-6708/2004/11/040 arXiv:hep-ph/0409146
44. S. Frixione, P. Nason, C. Oleari, Matching NLO QCD computations with parton shower simulations: the POWHEG method. JHEP **11**, 070 (2007). https://doi.org/10.1088/1126-6708/2007/11/070 arXiv:0709.2092 [hep-ph]
45. S. Alioli, P. Nason, C. Oleari, E. Re, A general framework for implementing NLO calculations in shower Monte Carlo programs: the POWHEG BOX. JHEP **06**, 043 (2010). https://doi.org/10.1007/JHEP06(2010)043 arXiv:1002.2581 [hep-ph]
46. T. Sjöstrand et al., An introduction to PYTHIA 8.2. Comput. Phys. Commun. **191**, 159 (2015). https://doi.org/10.1016/j.cpc.2015.01.024 arXiv:1410.3012 [hep-ph]
47. ATLAS Collaboration, ATLAS Pythia 8 tunes to 7 TeV data. ATL-PHYS-PUB-2014-021 (2014). https://cds.cern.ch/record/1966419
48. R.D. Ball et al., Parton distributions with LHC data. Nucl. Phys. B **867**, 244 (2013). https://doi.org/10.1016/j.nuclphysb.2012.10.003 arXiv:1207.1303 [hep-ph]
49. D.J. Lange, The EvtGen particle decay simulation package. Nucl. Instrum. Methods A **462**, 152 (2001). https://doi.org/10.1016/S0168-9002(01)00089-4
50. ATLAS Collaboration, Studies on top-quark Monte Carlo modelling for Top2016. ATL-PHYS-PUB-2016-020 (2016). https://cds.cern.ch/record/2216168
51. M. Beneke, P. Falgari, S. Klein, C. Schwinn, Hadronic top-quark pair production with NNLL threshold resummation. Nucl. Phys. B **855**, 695 (2012). https://doi.org/10.1016/j.nuclphysb.2011.10.021 arXiv:1109.1536 [hep-ph]
52. M. Cacciari, M. Czakon, M. Mangano, A. Mitov, P. Nason, Top-pair production at hadron colliders with next-to-next-to-leading logarithmic soft-gluon resummation. Phys. Lett. B **710**, 612 (2012). https://doi.org/10.1016/j.physletb.2012.03.013 arXiv:1111.5869 [hep-ph]
53. P. Bärnreuther, M. Czakon, A. Mitov, Percent-level-precision physics at the Tevatron: next-to-next-to-leading order QCD corrections to $q\bar{q} \to t\bar{t} + X$. Phys. Rev. Lett. **109**, 132001 (2012). https://doi.org/10.1103/PhysRevLett.109.132001 arXiv:1204.5201 [hep-ph]
54. M. Czakon, A. Mitov, NNLO corrections to top-pair production at hadron colliders: the all-fermionic scattering channels. JHEP **12**, 054 (2012). https://doi.org/10.1007/JHEP12(2012)054 arXiv:1207.0236 [hep-ph]
55. M. Czakon, A. Mitov, NNLO corrections to top pair production at hadron colliders: the quark-gluon reaction. JHEP **01**, 080 (2013). https://doi.org/10.1007/JHEP01(2013)080 arXiv:1210.6832 [hep-ph]
56. M. Czakon, P. Fiedler, A. Mitov, Total top-quark pair-production cross section at hadron colliders through $O(\alpha_S^4)$. Phys. Rev. Lett. **110**, 252004 (2013). https://doi.org/10.1103/PhysRevLett.110.252004 arXiv:1303.6254 [hep-ph]
57. M. Czakon, A. Mitov, Top++: a program for the calculation of the top-pair cross-section at hadron colliders. Comput. Phys. Commun. **185**, 2930 (2014). https://doi.org/10.1016/j.cpc.2014.06.021 arXiv:1112.5675 [hep-ph]
58. M. Aliev et al., HATHOR: HAdronic Top and Heavy quarks crOss section calculatoR. Comput. Phys. Commun. **182**, 1034 (2011). https://doi.org/10.1016/j.cpc.2010.12.040 arXiv:1007.1327 [hep-ph]
59. P. Kant et al., HatHor for single top-quark production: updated predictions and uncertainty estimates for single top-quark production in hadronic collisions. Comput. Phys. Commun. **191**, 74 (2015). https://doi.org/10.1016/j.cpc.2015.02.001 arXiv:1406.4403 [hep-ph]
60. S. Frixione, E. Laenen, P. Motylinski, C. White, B.R. Webber, Single-top hadroproduction in association with a W boson. JHEP **07**, 029 (2008). https://doi.org/10.1088/1126-6708/2008/07/029 arXiv:0805.3067 [hep-ph]
61. J. Alwall et al., The automated computation of tree-level and next-to-leading order differential cross sections, and their matching to parton shower simulations. JHEP **07**, 079 (2014). https://doi.org/10.1007/JHEP07(2014)079 arXiv:1405.0301 [hep-ph]
62. T. Sjöstrand, S. Mrenna, P. Skands, A brief introduction to PYTHIA 8.1. Comput. Phys. Commun. **178**, 852 (2008). https://doi.org/10.1016/j.cpc.2008.01.036 arXiv:0710.3820 [hep-ph]
63. L. Lönnblad, Correcting the colour-dipole cascade model with fixed order matrix elements. JHEP **05**, 046 (2002). https://doi.org/10.1088/1126-6708/2002/05/046 arXiv:hep-ph/0112284
64. L. Lönnblad, S. Prestel, Matching tree-level matrix elements with interleaved showers. JHEP **03**, 019 (2012). https://doi.org/10.1007/JHEP03(2012)019 arXiv:1109.4829 [hep-ph]
65. ATLAS Collaboration, The ATLAS simulation infrastructure. Eur. Phys. J. C **70**, 823 (2010). https://doi.org/10.1140/epjc/s10052-010-1429-9. arXiv:1005.4568 [physics.ins-det]
66. GEANT4 Collaboration, S. Agostinelli et al., Geant4—a simulation toolkit. Nucl. Instrum. Methods A **506**, 250 (2003). https://doi.org/10.1016/S0168-9002(03)01368-8
67. M.P. Guthrie, R.G. Alsmiller, H.W. Bertini, Calculation of the capture of negative pions in light elements and comparison with experiments pertaining to cancer radiotherapy. Nucl. Instrum. Methods **66**, 29 (1968). https://doi.org/10.1016/0029-554X(68)90054-2
68. B. Andersson, G. Gustafson, B. Nilsson-Almqvist, A model for low-pT hadronic reactions with generalizations to hadron–nucleus and nucleus–nucleus collisions. Nucl. Phys. B **281**, 289 (1987). https://doi.org/10.1016/0550-3213(87)90257-4. ISSN:0550-3213
69. B. Nilsson-Almqvist, E. Stenlund, Interactions between hadrons and nuclei: the Lund Monte Carlo—FRITIOF version 1.6. Comput. Phys. Commun. **43**, 387 (1987). https://doi.org/10.1016/0010-4655(87)90056-7. ISSN:0010-4655
70. ATLAS Collaboration, The Pythia 8 A3 tune description of ATLAS minimum bias and inelastic measurements incorporating the Donnachie–Landshoff diffractive model. ATL-PHYS-PUB-2016-017 (2016). https://cds.cern.ch/record/2206965
71. ATLAS Collaboration, Performance of the ATLAS track reconstruction algorithms in dense environments in LHC Run 2. Eur. Phys. J. C **77**, 673 (2017). https://doi.org/10.1140/epjc/s10052-017-5225-7. arXiv:1704.07983 [hep-ex]
72. ATLAS Collaboration, Early inner detector tracking performance in the 2015 data at $\sqrt{s} = 13$ TeV. ATL-PHYS-PUB-2015-051 (2015). https://cds.cern.ch/record/2110140
73. ATLAS Collaboration, Topological cell clustering in the ATLAS calorimeters and its performance in LHC Run 1. Eur. Phys. J. C **77**, 490 (2017). https://doi.org/10.1140/epjc/s10052-017-5004-5. arXiv:1603.02934 [hep-ex]
74. ATLAS Collaboration, Electron and photon performance measurements with the ATLAS detector using the 2015–2017 LHC proton–proton collision data. JINST **14**, P12006 (2019). https://doi.org/10.1088/1748-0221/14/12/P12006. arXiv:1908.00005 [hep-ex]

75. ATLAS Collaboration, Muon reconstruction and identification efficiency in ATLAS using the full Run 2 pp collision data set at $\sqrt{s} = 13$ TeV. Eur. Phys. J. C **81**, 578 (2020). https://doi.org/10.1140/epjc/s10052-021-09233-2. arXiv:2012.00578 [hep-ex]
76. ATLAS Collaboration, Muon reconstruction performance of the ATLAS detector in proton–proton collision data at $\sqrt{s} = 13$ TeV. Eur. Phys. J. C **76**, 292 (2016). https://doi.org/10.1140/epjc/s10052-016-4120-y. arXiv:1603.05598 [hep-ex]
77. M. Cacciari, G.P. Salam, G. Soyez, The anti-k_t jet clustering algorithm. JHEP **04**, 063 (2008). https://doi.org/10.1088/1126-6708/2008/04/063 arXiv:0802.1189 [hep-ph]
78. M. Cacciari, G.P. Salam, G. Soyez, FastJet user manual. Eur. Phys. J. C **72**, 1896 (2012). https://doi.org/10.1140/epjc/s10052-012-1896-2 arXiv:1111.6097 [hep-ph]
79. ATLAS Collaboration, Performance of pile-up mitigation techniques for jets in pp collisions at $\sqrt{s} = 8$ TeV using the ATLAS detector. Eur. Phys. J. C **76**, 581 (2016). https://doi.org/10.1140/epjc/s10052-016-4395-z. arXiv:1510.03823 [hep-ex]
80. ATLAS Collaboration, Reconstruction of primary vertices at the ATLAS experiment in Run 1 proton–proton collisions at the LHC. Eur. Phys. J. C **77**, 332 (2017). https://doi.org/10.1140/epjc/s10052-017-4887-5. arXiv:1611.10235 [hep-ex]
81. ATLAS Collaboration, Performance of missing transverse momentum reconstruction with the ATLAS detector using proton–proton collisions at $\sqrt{s} = 13$ TeV. Eur. Phys. J. C **78**, 903 (2018). https://doi.org/10.1140/epjc/s10052-018-6288-9. arXiv:1802.08168 [hep-ex]
82. ATLAS Collaboration, Performance of the ATLAS inner detector track and vertex reconstruction in high pile-up LHC environment. ATLAS-CONF-2012-042 (2012). https://cds.cern.ch/record/1435196
83. M. Cacciari, G.P. Salam, Pileup subtraction using jet areas. Phys. Lett. B **659**, 119 (2008). https://doi.org/10.1016/j.physletb.2007.09.077 arXiv:0707.1378 [hep-ph]
84. L.D. Landau, On the energy loss of fast particles by ionization. J. Phys. (USSR) **8**, 201 (1944)
85. ATLAS Collaboration, Measurement of the muon reconstruction performance of the ATLAS detector using 2011 and 2012 LHC proton–proton collision data. Eur. Phys. J. C **74**, 3130 (2014). https://doi.org/10.1140/epjc/s10052-014-3130-x. arXiv:1407.3935 [hep-ex]
86. J.H. Friedman, Data analysis techniques for high energy particle physics. CERN-1974-023.271 (1974). http://cds.cern.ch/record/695770
87. ATLAS Collaboration, Jet energy measurement and its systematic uncertainty in proton–proton collisions at $\sqrt{s} = 7$ TeV with the ATLAS detector. Eur. Phys. J. C **75**, 17 (2015). https://doi.org/10.1140/epjc/s10052-014-3190-y. arXiv:1406.0076 [hep-ex]
88. ATLAS Collaboration, ATLAS computing acknowledgements. ATL-SOFT-PUB-2021-003 (2021). https://cds.cern.ch/record/2776662

ATLAS Collaboration

G. Aad[98], B. Abbott[123], D. C. Abbott[99], A. Abed Abud[34], K. Abeling[51], D. K. Abhayasinghe[91], S. H. Abidi[27], A. Aboulhorma[33e], H. Abramowicz[156], H. Abreu[155], Y. Abulaiti[5], A. C. Abusleme Hoffman[141a], B. S. Acharya[64a,64b,o], B. Achkar[51], L. Adam[96], C. Adam Bourdarios[4], L. Adamczyk[81a], L. Adamek[161], S. V. Addepalli[24], J. Adelman[116], A. Adiguzel[11c,ac], S. Adorni[52], T. Adye[138], A. A. Affolder[140], Y. Afik[34], C. Agapopoulou[62], M. N. Agaras[12], J. Agarwala[68a,68b], A. Aggarwal[114], C. Agheorghiesei[25c], J. A. Aguilar-Saavedra[134a,134f,ab], A. Ahmad[34], F. Ahmadov[77], W. S. Ahmed[100], X. Ai[44], G. Aielli[71a,71b], I. Aizenberg[174], S. Akatsuka[83], M. Akbiyik[96], T. P. A. Åkesson[94], A. V. Akimov[107], K. Al Khoury[37], G. L. Alberghi[21b], J. Albert[170], P. Albicocco[49], M. J. Alconada Verzini[86], S. Alderweireldt[48], M. Aleksa[34], I. N. Aleksandrov[77], C. Alexa[25b], T. Alexopoulos[9], A. Alfonsi[115], F. Alfonsi[21b], M. Alhroob[123], B. Ali[136], S. Ali[153], M. Aliev[160], G. Alimonti[66a], C. Allaire[34], B. M. M. Allbrooke[151], P. P. Allport[19], A. Aloisio[67a,67b], F. Alonso[86], C. Alpigiani[143], E. Alunno Camelia[71a,71b], M. Alvarez Estevez[95], M. G. Alviggi[67a,67b], Y. Amaral Coutinho[78b], A. Ambler[100], L. Ambroz[129], C. Amelung[34], D. Amidei[102], S. P. Amor Dos Santos[134a], S. Amoroso[44], C. S. Amrouche[52], C. Anastopoulos[144], N. Andari[139], T. Andeen[10], J. K. Anders[18], S. Y. Andrean[43a,43b], A. Andreazza[66a,66b], S. Angelidakis[8], A. Angerami[37], A. V. Anisenkov[117a,117b], A. Annovi[69a], C. Antel[52], M. T. Anthony[144], E. Antipov[124], M. Antonelli[49], D. J. A. Antrim[16], F. Anulli[70a], M. Aoki[79], J. A. Aparisi Pozo[168], M. A. Aparo[151], L. Aperio Bella[44], N. Aranzabal[34], V. Araujo Ferraz[78a], C. Arcangeletti[49], A. T. H. Arce[47], E. Arena[88], J-F. Arguin[106], S. Argyropoulos[50], J.-H. Arling[44], A. J. Armbruster[34], A. Armstrong[165], O. Arnaez[161], H. Arnold[34], Z. P. Arrubarrena Tame[110], G. Artoni[129], H. Asada[112], K. Asai[121], S. Asai[158], N. A. Asbah[57], E. M. Asimakopoulou[166], L. Asquith[151], J. Assahsah[33d], K. Assamagan[27], R. Astalos[26a], R. J. Atkin[31a], M. Atkinson[167], N. B. Atlay[17], H. Atmani[58b], P. A. Atmasiddha[102], K. Augsten[136], S. Auricchio[67a,67b], V. A. Austrup[176], G. Avner[155], G. Avolio[34], M. K. Ayoub[13c], G. Azuelos[106,aj], D. Babal[26a], H. Bachacou[139], K. Bachas[157], A. Bachiu[32], F. Backman[43a,43b], A. Badea[57], P. Bagnaia[70a,70b], H. Bahrasemani[147], A. J. Bailey[168], V. R. Bailey[167], J. T. Baines[138], C. Bakalis[9], O. K. Baker[177], P. J. Bakker[115], E. Bakos[14], D. Bakshi Gupta[7], S. Balaji[152], R. Balasubramanian[115], E. M. Baldin[117a,117b], P. Balek[137], E. Ballabene[66a,66b], F. Balli[139], W. K. Balunas[129], J. Balz[96], E. Banas[82], M. Bandieramonte[133], A. Bandyopadhyay[17], S. Bansal[22], L. Barak[156], E. L. Barberio[101], D. Barberis[53a,53b], M. Barbero[98], G. Barbour[92], K. N. Barends[31a], T. Barillari[111], M-S. Barisits[34], J. Barkeloo[126], T. Barklow[148], B. M. Barnett[138],

R. M. Barnett[16], A. Baroncelli[58a], G. Barone[27], A. J. Barr[129], L. Barranco Navarro[43a,43b], F. Barreiro[95], J. Barreiro Guimarães da Costa[13a], U. Barron[156], S. Barsov[132], F. Bartels[59a], R. Bartoldus[148], G. Bartolini[98], A. E. Barton[87], P. Bartos[26a], A. Basalaev[44], A. Basan[96], M. Baselga[44], I. Bashta[72a,72b], A. Bassalat[62,ag], M. J. Basso[161], C. R. Basson[97], R. L. Bates[55], S. Batlamous[33e], J. R. Batley[30], B. Batool[146], M. Battaglia[140], M. Bauce[70a,70b], F. Bauer[139,*], P. Bauer[22], H. S. Bawa[29], A. Bayirli[11c], J. B. Beacham[47], T. Beau[130], P. H. Beauchemin[164], F. Becherer[50], P. Bechtle[22], H. P. Beck[18,q], K. Becker[172], C. Becot[44], A. J. Beddall[11a], V. A. Bednyakov[77], C. P. Bee[150], T. A. Beermann[34], M. Begalli[78b], M. Begel[27], A. Behera[150], J. K. Behr[44], C. Beirao Da Cruz E Silva[34], J. F. Beirer[34,51], F. Beisiegel[22], M. Belfkir[4], G. Bella[156], L. Bellagamba[21b], A. Bellerive[32], P. Bellos[19], K. Beloborodov[117a,117b], K. Belotskiy[108], N. L. Belyaev[108], D. Benchekroun[33a], Y. Benhammou[156], D. P. Benjamin[27], M. Benoit[27], J. R. Bensinger[24], S. Bentvelsen[115], L. Beresford[34], M. Beretta[49], D. Berge[17], E. Bergeaas Kuutmann[166], N. Berger[4], B. Bergmann[136], L. J. Bergsten[24], J. Beringer[16], S. Berlendis[6], G. Bernardi[130], C. Bernius[148], F. U. Bernlochner[22], T. Berry[91], P. Berta[137], A. Berthold[46], I. A. Bertram[87], O. Bessidskaia Bylund[176], S. Bethke[111], A. Betti[40], A. J. Bevan[90], S. Bhatta[150], D. S. Bhattacharya[171], P. Bhattarai[24], V. S. Bhopatkar[5], R. Bi[133], R. M. Bianchi[133], O. Biebel[110], R. Bielski[126], N. V. Biesuz[69a,69b], M. Biglietti[72a], T. R. V. Billoud[136], M. Bindi[51], A. Bingul[11d], C. Bini[70a,70b], S. Biondi[21a,21b], A. Biondini[88], C. J. Birch-sykes[97], G. A. Bird[19,138], M. Birman[174], T. Bisanz[34], J. P. Biswal[2], D. Biswas[175,j], A. Bitadze[97], C. Bittrich[46], K. Bjørke[128], I. Bloch[44], C. Blocker[24], A. Blue[55], U. Blumenschein[90], J. Blumenthal[96], G. J. Bobbink[115], V. S. Bobrovnikov[117a,117b], M. Boehler[50], D. Bogavac[12], A. G. Bogdanchikov[117a,117b], C. Bohm[43a], V. Boisvert[91], P. Bokan[44], T. Bold[81a], M. Bomben[130], M. Bona[90], M. Boonekamp[139], C. D. Booth[91], A. G. Borbély[55], H. M. Borecka-Bielska[106], L. S. Borgna[92], G. Borissov[87], D. Bortoletto[129], D. Boscherini[21b], M. Bosman[12], J. D. Bossio Sola[34], K. Bouaouda[33a], J. Boudreau[133], E. V. Bouhova-Thacker[87], D. Boumediene[36], R. Bouquet[130], A. Boveia[122], J. Boyd[34], D. Boye[27], I. R. Boyko[77], A. J. Bozson[91], J. Bracinik[19], N. Brahimi[58c,58d], G. Brandt[176], O. Brandt[30], F. Braren[44], B. Brau[99], J. E. Brau[126], W. D. Breaden Madden[55], K. Brendlinger[44], R. Brener[174], L. Brenner[34], R. Brenner[166], S. Bressler[174], B. Brickwedde[96], D. L. Briglin[19], D. Britton[55], D. Britzger[111], I. Brock[22], R. Brock[103], G. Brooijmans[37], W. K. Brooks[141d], E. Brost[27], P. A. Bruckman de Renstrom[82], B. Brüers[44], D. Bruncko[26b], A. Bruni[21b], G. Bruni[21b], M. Bruschi[21b], N. Bruscino[70a,70b], L. Bryngemark[148], T. Buanes[15], Q. Buat[150], P. Buchholz[146], A. G. Buckley[55], I. A. Budagov[77], M. K. Bugge[128], O. Bulekov[108], B. A. Bullard[57], S. Burdin[88], C. D. Burgard[44], A. M. Burger[124], B. Burghgrave[7], J. T. P. Burr[44], C. D. Burton[10], J. C. Burzynski[99], E. L. Busch[37], V. Büscher[96], P. J. Bussey[55], J. M. Butler[23], C. M. Buttar[55], J. M. Butterworth[92], W. Buttinger[138], C. J. Buxo Vazquez[103], A. R. Buzykaev[117a,117b], G. Cabras[21b], S. Cabrera Urbán[168], D. Caforio[54], H. Cai[133], V. M. M. Cairo[148], O. Cakir[3a], N. Calace[34], P. Calafiura[16], G. Calderini[130], P. Calfayan[63], G. Callea[55], L. P. Caloba[78b], S. Calvente Lopez[95], D. Calvet[36], S. Calvet[36], T. P. Calvet[98], M. Calvetti[69a,69b], R. Camacho Toro[130], S. Camarda[34], D. Camarero Munoz[95], P. Camarri[71a,71b], M. T. Camerlingo[72a,72b], D. Cameron[128], C. Camincher[170], M. Campanelli[92], A. Camplani[38], V. Canale[67a,67b], A. Canesse[100], M. Cano Bret[75], J. Cantero[124], Y. Cao[167], F. Capocasa[24], M. Capua[39a,39b], A. Carbone[66a,66b], R. Cardarelli[71a], J. C. J. Cardenas[7], F. Cardillo[168], G. Carducci[39a,39b], T. Carli[34], G. Carlino[67a], B. T. Carlson[133], E. M. Carlson[162a,170], L. Carminati[66a,66b], M. Carnesale[70a,70b], R. M. D. Carney[148], S. Caron[114], E. Carquin[141d], S. Carrá[44], G. Carratta[21a,21b], J. W. S. Carter[161], T. M. Carter[48], D. Casadei[31c], M. P. Casado[12,g], A. F. Casha[161], E. G. Castiglia[177], F. L. Castillo[59a], L. Castillo Garcia[12], V. Castillo Gimenez[168], N. F. Castro[134a,134e], A. Catinaccio[34], J. R. Catmore[128], A. Cattai[34], V. Cavaliere[27], N. Cavalli[21a,21b], V. Cavasinni[69a,69b], E. Celebi[11b], F. Celli[129], M. S. Centonze[65a,65b], K. Cerny[125], A. S. Cerqueira[78a], A. Cerri[151], L. Cerrito[71a,71b], F. Cerutti[16], A. Cervelli[21b], S. A. Cetin[11b], Z. Chadi[33a], D. Chakraborty[116], M. Chala[134f], J. Chan[175], W. S. Chan[115], W. Y. Chan[88], J. D. Chapman[30], B. Chargeishvili[154b], D. G. Charlton[19], T. P. Charman[90], M. Chatterjee[18], S. Chekanov[5], S. V. Chekulaev[162a], G. A. Chelkov[77,ae], A. Chen[102], B. Chen[156], B. Chen[170], C. Chen[58a], C. H. Chen[76], H. Chen[13c], H. Chen[27], J. Chen[58c], J. Chen[24], S. Chen[131], S. J. Chen[13c], X. Chen[58c], X. Chen[13b], Y. Chen[58a], Y-H. Chen[44], C. L. Cheng[175], H. C. Cheng[60a], A. Cheplakov[77], E. Cheremushkina[44], E. Cherepanova[77], R. Cherkaoui El Moursli[33e], E. Cheu[6], K. Cheung[61], L. Chevalier[139], V. Chiarella[49], G. Chiarelli[69a], G. Chiodini[65a], A. S. Chisholm[19], A. Chitan[25b], Y. H. Chiu[170], M. V. Chizhov[77,s], K. Choi[10], A. R. Chomont[70a,70b], Y. Chou[99], Y. S. Chow[115], T. Chowdhury[31f], L. D. Christopher[31f], M. C. Chu[60a], X. Chu[13a,13d], J. Chudoba[135], J. J. Chwastowski[82], D. Cieri[111], K. M. Ciesla[82], V. Cindro[89], I. A. Cioară[25b], A. Ciocio[16], F. Cirotto[67a,67b], Z. H. Citron[174,k],

M. Citterio[66a], D. A. Ciubotaru[25b], B. M. Ciungu[161], A. Clark[52], P. J. Clark[48], J. M. Clavijo Columbie[44], S. E. Clawson[97], C. Clement[43a,43b], L. Clissa[21a,21b], Y. Coadou[98], M. Cobal[64a,64c], A. Coccaro[53b], J. Cochran[76], R. F. Coelho Barrue[134a], R. Coelho Lopes De Sa[99], S. Coelli[66a], H. Cohen[156], A. E. C. Coimbra[34], B. Cole[37], J. Collot[56], P. Conde Muiño[134a,134h], S. H. Connell[31c], I. A. Connelly[55], E. I. Conroy[129], F. Conventi[67a,ak], H. G. Cooke[19], A. M. Cooper-Sarkar[129], F. Cormier[169], L. D. Corpe[34], M. Corradi[70a,70b], E. E. Corrigan[94], F. Corriveau[100,y], M. J. Costa[168], F. Costanza[4], D. Costanzo[144], B. M. Cote[122], G. Cowan[91], J. W. Cowley[30], K. Cranmer[120], S. Crépé-Renaudin[56], F. Crescioli[130], M. Cristinziani[146], M. Cristoforetti[73a,73b,b], V. Croft[164], G. Crosetti[39a,39b], A. Cueto[34], T. Cuhadar Donszelmann[165], H. Cui[13a,13d], A. R. Cukierman[148], W. R. Cunningham[55], F. Curcio[39a,39b], P. Czodrowski[34], M. M. Czurylo[59b], M. J. Da Cunha Sargedas De Sousa[58a], J. V. Da Fonseca Pinto[78b], C. Da Via[97], W. Dabrowski[81a], T. Dado[45], S. Dahbi[31f], T. Dai[102], C. Dallapiccola[99], M. Dam[38], G. D'amen[27], V. D'Amico[72a,72b], J. Damp[96], J. R. Dandoy[131], M. F. Daneri[28], M. Danninger[147], V. Dao[34], G. Darbo[53b], S. Darmora[5], A. Dattagupta[126], S. D'Auria[66a,66b], C. David[162b], T. Davidek[137], D. R. Davis[47], B. Davis-Purcell[32], I. Dawson[90], K. De[7], R. De Asmundis[67a], M. De Beurs[115], S. De Castro[21a,21b], N. De Groot[114], P. de Jong[115], H. De la Torre[103], A. De Maria[13c], D. De Pedis[70a], A. De Salvo[70a], U. De Sanctis[71a,71b], M. De Santis[71a,71b], A. De Santo[151], J. B. De Vivie De Regie[56], D. V. Dedovich[77], J. Degens[115], A. M. Deiana[40], J. Del Peso[95], Y. Delabat Diaz[44], F. Deliot[139], C. M. Delitzsch[6], M. Della Pietra[67a,67b], D. Della Volpe[52], A. Dell'Acqua[34], L. Dell'Asta[66a,66b], M. Delmastro[4], P. A. Delsart[56], S. Demers[177], M. Demichev[77], S. P. Denisov[118], L. D'Eramo[116], D. Derendarz[82], J. E. Derkaoui[33d], F. Derue[130], P. Dervan[88], K. Desch[22], K. Dette[161], C. Deutsch[22], P. O. Deviveiros[34], F. A. Di Bello[70a,70b], A. Di Ciaccio[71a,71b], L. Di Ciaccio[4], A. Di Domenico[70a,70b], C. Di Donato[67a,67b], A. Di Girolamo[34], G. Di Gregorio[69a,69b], A. Di Luca[73a,73b], B. Di Micco[72a,72b], R. Di Nardo[72a,72b], C. Diaconu[98], F. A. Dias[115], T. Dias Do Vale[134a], M. A. Diaz[141a], F. G. Diaz Capriles[22], J. Dickinson[16], M. Didenko[168], E. B. Diehl[102], J. Dietrich[17], S. Díez Cornell[44], C. Diez Pardos[146], A. Dimitrievska[16], W. Ding[13b], J. Dingfelder[22], I-M. Dinu[25b], S. J. Dittmeier[59b], F. Dittus[34], F. Djama[98], T. Djobava[154b], J. I. Djuvsland[15], M. A. B. Do Vale[142], D. Dodsworth[24], C. Doglioni[94], J. Dolejsi[137], Z. Dolezal[137], M. Donadelli[78c], B. Dong[58c], J. Donini[36], A. D'onofrio[13c], M. D'Onofrio[88], J. Dopke[138], A. Doria[67a], M. T. Dova[86], A. T. Doyle[55], E. Drechsler[147], E. Dreyer[147], T. Dreyer[51], A. S. Drobac[164], D. Du[58a], T. A. du Pree[115], F. Dubinin[107], M. Dubovsky[26a], A. Dubreuil[52], E. Duchovni[174], G. Duckeck[110], O. A. Ducu[25b,34], D. Duda[111], A. Dudarev[34], M. D'uffizi[97], L. Duflot[62], M. Dührssen[34], C. Dülsen[176], A. E. Dumitriu[25b], M. Dunford[59a], S. Dungs[45], K. Dunne[43a,43b], A. Duperrin[98], H. Duran Yildiz[3a], M. Düren[54], A. Durglishvili[154b], B. Dutta[44], G. I. Dyckes[16], M. Dyndal[81a], S. Dysch[97], B. S. Dziedzic[82], B. Eckerova[26a], M. G. Eggleston[47], E. Egidio Purcino De Souza[78b], L. F. Ehrke[52], T. Eifert[7], G. Eigen[15], K. Einsweiler[16], T. Ekelof[166], Y. El Ghazali[33b], H. El Jarrari[33e], A. El Moussaouy[33a], V. Ellajosyula[166], M. Ellert[166], F. Ellinghaus[176], A. A. Elliot[90], N. Ellis[34], J. Elmsheuser[27], M. Elsing[34], D. Emeliyanov[138], A. Emerman[37], Y. Enari[158], J. Erdmann[45], A. Ereditato[18], P. A. Erland[82], M. Errenst[176], M. Escalier[62], C. Escobar[168], O. Estrada Pastor[168], E. Etzion[156], G. Evans[134a], H. Evans[63], M. O. Evans[151], A. Ezhilov[132], F. Fabbri[55], L. Fabbri[21a,21b], G. Facini[172], V. Fadeyev[140], R. M. Fakhrutdinov[118], S. Falciano[70a], P. J. Falke[22], S. Falke[34], J. Faltova[137], Y. Fan[13a], Y. Fang[13a], Y. Fang[13a], G. Fanourakis[42], M. Fanti[66a,66b], M. Faraj[58c], A. Farbin[7], A. Farilla[72a], E. M. Farina[68a,68b], T. Farooque[103], S. M. Farrington[48], P. Farthouat[34], F. Fassi[33e], D. Fassouliotis[8], M. Faucci Giannelli[71a,71b], W. J. Fawcett[30], L. Fayard[62], O. L. Fedin[132,p], M. Feickert[167], L. Feligioni[98], A. Fell[144], C. Feng[58b], M. Feng[13b], M. J. Fenton[165], A. B. Fenyuk[118], S. W. Ferguson[41], J. Ferrando[44], A. Ferrari[166], P. Ferrari[115], R. Ferrari[68a], D. Ferrere[52], C. Ferretti[102], F. Fiedler[96], A. Filipčič[89], F. Filthaut[114], M. C. N. Fiolhais[134a,134c,a], L. Fiorini[168], F. Fi scher[146], W. C. Fisher[103], T. Fitschen[19], I. Fleck[146], P. Fleischmann[102], T. Flick[176], B. M. Flierl[110], L. Flores[131], M. Flores[31f], L. R. Flores Castillo[60a], F. M. Follega[73a,73b], N. Fomin[15], J. H. Foo[161], B. C. Forland[63], A. Formica[139], F. A. Förster[12], A. C. Forti[97], E. Fortin[98], M. G. Foti[129], L. Fountas[8], D. Fournier[62], H. Fox[87], P. Francavilla[69a,69b], S. Francescato[57], M. Franchini[21a,21b], S. Franchino[59a], D. Francis[34], L. Franco[4], L. Franconi[18], M. Franklin[57], G. Frattari[70a,70b], A. C. Freegard[90], P. M. Freeman[19], W. S. Freund[78b], E. M. Freundlich[45], D. Froidevaux[34], J. A. Frost[129], Y. Fu[58a], M. Fujimoto[121], E. Fullana Torregrosa[168], J. Fuster[168], A. Gabrielli[21a,21b], A. Gabrielli[34], P. Gadow[44], G. Gagliardi[53a,53b], L. G. Gagnon[16], G. E. Gallardo[129], E. J. Gallas[129], B. J. Gallop[138], R. Gamboa Goni[90], K. K. Gan[122], S. Ganguly[174], J. Gao[58a], Y. Gao[48], Y. S. Gao[29,m], F. M. Garay Walls[141a], C. García[168], J. E. García Navarro[168], J. A. García Pascual[13a],

M. Garcia-Sciveres[16], R. W. Gardner[35], D. Garg[75], R. B. Garg[148], S. Gargiulo[50], C. A. Garner[161], V. Garonne[128], S. J. Gasiorowski[143], P. Gaspar[78b], G. Gaudio[68a], P. Gauzzi[70a,70b], I. L. Gavrilenko[107], A. Gavrilyuk[119], C. Gay[169], G. Gaycken[44], E. N. Gazis[9], A. A. Geanta[25b], C. M. Gee[140], C. N. P. Gee[138], J. Geisen[94], M. Geisen[96], C. Gemme[53b], M. H. Genest[56], S. Gentile[70a,70b], S. George[91], W. F. George[19], T. Geralis[42], L. O. Gerlach[51], P. Gessinger-Befurt[34], M. Ghasemi Bostanabad[170], M. Ghneimat[146], A. Ghosh[165], A. Ghosh[75], B. Giacobbe[21b], S. Giagu[70a,70b], N. Giangiacomi[161], P. Giannetti[69a], A. Giannini[67a,67b], S. M. Gibson[91], M. Gignac[140], D. T. Gil[81b], B. J. Gilbert[37], D. Gillberg[32], G. Gilles[115], N. E. K. Gillwald[44], D. M. Gingrich[2,aj], M. P. Giordani[64a,64c], P. F. Giraud[139], G. Giugliarelli[64a,64c], D. Giugni[66a], F. Giuli[71a,71b], I. Gkialas[8,h], P. Gkountoumis[9], L. K. Gladilin[109], C. Glasman[95], G. R. Gledhill[126], M. Glisic[126], I. Gnesi[39b,d], M. Goblirsch-Kolb[24], D. Godin[106], S. Goldfarb[101], T. Golling[52], D. Golubkov[118], J. P. Gombas[103], A. Gomes[134a,134b], R. Goncalves Gama[51], R. Gonçalo[134a,134c], G. Gonella[126], L. Gonella[19], A. Gongadze[77], F. Gonnella[19], J. L. Gonski[37], S. González de la Hoz[168], S. Gonzalez Fernandez[12], R. Gonzalez Lopez[88], C. Gonzalez Renteria[16], R. Gonzalez Suarez[166], S. Gonzalez-Sevilla[52], G. R. Gonzalvo Rodriguez[168], R.Y. González Andana[141a], L. Goossens[34], N. A. Gorasia[19], P. A. Gorbounov[119], H. A. Gordon[27], B. Gorini[34], E. Gorini[65a,65b], A. Gorišek[89], A. T. Goshaw[47], M. I. Gostkin[77], C. A. Gottardo[114], M. Gouighri[33b], V. Goumarre[44], A. G. Goussiou[143], N. Govender[31c], C. Goy[4], I. Grabowska-Bold[81a], K. Graham[32], E. Gramstad[128], S. Grancagnolo[17], M. Grandi[151], V. Gratchev[132], P. M. Gravila[25f], F. G. Gravili[65a,65b], H. M. Gray[16], C. Grefe[22], I. M. Gregor[44], P. Grenier[148], K. Grevtsov[44], C. Grieco[12], N. A. Grieser[123], A. A. Grillo[140], K. Grimm[29,l], S. Grinstein[12,v], J.-F. Grivaz[62], S. Groh[96], E. Gross[174], J. Grosse-Knetter[51], C. Grud[102], A. Grummer[113], J. C. Grundy[129], L. Guan[102], W. Guan[175], C. Gubbels[169], J. Guenther[34], J. G. R. Guerrero Rojas[168], F. Guescini[111], D. Guest[17], R. Gugel[96], A. Guida[44], T. Guillemin[4], S. Guindon[34], J. Guo[58c], L. Guo[62], Y. Guo[102], R. Gupta[44], S. Gurbuz[22], G. Gustavino[123], M. Guth[52], P. Gutierrez[123], L. F. Gutierrez Zagazeta[131], C. Gutschow[92], C. Guyot[139], C. Gwenlan[129], C. B. Gwilliam[88], E. S. Haaland[128], A. Haas[120], M. Habedank[17], C. Haber[16], H. K. Hadavand[7], A. Hadef[96], S. Hadzic[111], M. Haleem[171], J. Haley[124], J. J. Hall[144], G. Halladjian[103], G. D. Hallewell[98], L. Halser[18], K. Hamano[170], H. Hamdaoui[33e], M. Hamer[22], G. N. Hamity[48], K. Han[58a], L. Han[13c], L. Han[58a], S. Han[16], Y. F. Han[161], K. Hanagaki[79,t], M. Hance[140], M. D. Hank[35], R. Hankache[97], E. Hansen[94], J. B. Hansen[38], J. D. Hansen[38], M. C. Hansen[22], P. H. Hansen[38], K. Hara[163], T. Harenberg[176], S. Harkusha[104], Y. T. Harris[129], P. F. Harrison[172], N. M. Hartman[148], N. M. Hartmann[110], Y. Hasegawa[145], A. Hasib[48], S. Hassani[139], S. Haug[18], R. Hauser[103], M. Havranek[136], C. M. Hawkes[19], R. J. Hawkings[34], S. Hayashida[112], D. Hayden[103], C. Hayes[102], R. L. Hayes[169], C. P. Hays[129], J. M. Hays[90], H. S. Hayward[88], S. J. Haywood[138], F. He[58a], Y. He[159], Y. He[130], M. P. Heath[48], V. Hedberg[94], A. L. Heggelund[128], N. D. Hehir[90], C. Heidegger[50], K. K. Heidegger[50], W. D. Heidorn[76], J. Heilman[32], S. Heim[44], T. Heim[16], B. Heinemann[44,ah], J. G. Heinlein[131], J. J. Heinrich[126], L. Heinrich[34], J. Hejbal[135], L. Helary[44], A. Held[120], C. M. Helling[140], S. Hellman[43a,43b], C. Helsens[34], R. C. W. Henderson[87], L. Henkelmann[30], A. M. Henriques Correia[34], H. Herde[148], Y. Hernández Jiménez[150], H. Herr[96], M. G. Herrmann[110], T. Herrmann[46], G. Herten[50], R. Hertenberger[110], L. Hervas[34], N. P. Hessey[162a], H. Hibi[80], S. Higashino[79], E. Higón-Rodriguez[168], K. H. Hiller[44], S. J. Hillier[19], M. Hils[46], I. Hinchliffe[16], F. Hinterkeuser[22], M. Hirose[127], S. Hirose[163], D. Hirschbuehl[176], B. Hiti[89], O. Hladik[135], J. Hobbs[150], R. Hobincu[25e], N. Hod[174], M. C. Hodgkinson[144], B. H. Hodkinson[30], A. Hoecker[34], J. Hofer[44], D. Hohn[50], T. Holm[22], T. R. Holmes[35], M. Holzbock[111], L. B. A. H. Hommels[30], B. P. Honan[97], J. Hong[58c], T. M. Hong[133], Y. Hong[51], J. C. Honig[50], A. Hönle[111], B. H. Hooberman[167], W. H. Hopkins[5], Y. Horii[112], L. A. Horyn[35], S. Hou[153], J. Howarth[55], J. Hoya[86], M. Hrabovsky[125], A. Hrynevich[105], T. Hryn'ova[4], P. J. Hsu[61], S.-C. Hsu[143], Q. Hu[37], S. Hu[58c], Y. F. Hu[13a,13d,al], D. P. Huang[92], X. Huang[13c], Y. Huang[58a], Y. Huang[13a], Z. Hubacek[136], F. Hubaut[98], M. Huebner[22], F. Huegging[22], T. B. Huffman[129], M. Huhtinen[34], S. K. Huiberts[15], R. Hulsken[56], N. Huseynov[77,z], J. Huston[103], J. Huth[57], R. Hyneman[148], S. Hyrych[26a], G. Iacobucci[52], G. Iakovidis[27], I. Ibragimov[146], L. Iconomidou-Fayard[62], P. Iengo[34], R. Iguchi[158], T. Iizawa[52], Y. Ikegami[79], A. Ilg[18], N. Ilic[161], H. Imam[33a], T. Ingebretsen Carlson[43a,43b], G. Introzzi[68a,68b], M. Iodice[72a], V. Ippolito[70a,70b], M. Ishino[158], W. Islam[175], C. Issever[17,44], S. Istin[11c,am], J. M. Iturbe Ponce[60a], R. Iuppa[73a,73b], A. Ivina[174], J. M. Izen[41], V. Izzo[67a], P. Jacka[135], P. Jackson[1], R. M. Jacobs[44], B. P. Jaeger[147], C. S. Jagfeld[110], G. Jäkel[176], K. Jakobs[50], T. Jakoubek[174], J. Jamieson[55], K. W. Janas[81a], G. Jarlskog[94], A. E. Jaspan[88], N. Javadov[77,z], T. Javůrek[34], M. Javurkova[99], F. Jeanneau[139], L. Jeanty[126], J. Jejelava[154a,aa], P. Jenni[50,e], S. Jézéquel[4], J. Jia[150], Z. Jia[13c], Y. Jiang[58a], S. Jiggins[48], J. Jimenez Pena[111], S. Jin[13c], A. Jinaru[25b],

O. Jinnouchi[159], H. Jivan[31f], P. Johansson[144], K. A. Johns[6], C. A. Johnson[63], D. M. Jones[30], E. Jones[172], R. W. L. Jones[87], T. J. Jones[88], J. Jovicevic[51], X. Ju[16], J. J. Junggeburth[34], A. Juste Rozas[12,v], S. Kabana[141c], A. Kaczmarska[82], M. Kado[70a,70b], H. Kagan[122], M. Kagan[148], A. Kahn[37], A. Kahn[131], C. Kahra[96], T. Kaji[173], E. Kajomovitz[155], C. W. Kalderon[27], A. Kamenshchikov[118], M. Kaneda[158], N. J. Kang[140], S. Kang[76], Y. Kano[112], J. Kanzaki[79], D. Kar[31f], K. Karava[129], M. J. Kareem[162b], I. Karkanias[157], S. N. Karpov[77], Z. M. Karpova[77], V. Kartvelishvili[87], A. N. Karyukhin[118], E. Kasimi[157], C. Kato[58d], J. Katzy[44], K. Kawade[145], K. Kawagoe[85], T. Kawaguchi[112], T. Kawamoto[139], G. Kawamura[51], E. F. Kay[170], F. I. Kaya[164], S. Kazakos[12], V. F. Kazanin[117a,117b], Y. Ke[150], J. M. Keaveney[31a], R. Keeler[170], J. S. Keller[32], D. Kelsey[151], J. J. Kempster[19], J. Kendrick[19], K. E. Kennedy[37], O. Kepka[135], S. Kersten[176], B. P. Kerševan[89], S. Ketabchi Haghighat[161], M. Khandoga[130], A. Khanov[124], A. G. Kharlamov[117a,117b], T. Kharlamova[117a,117b], E. E. Khoda[143], T. J. Khoo[17], G. Khoriauli[171], E. Khramov[77], J. Khubua[154b], S. Kido[80], M. Kiehn[34], A. Kilgallon[126], E. Kim[159], Y. K. Kim[35], N. Kimura[92], A. Kirchhoff[51], D. Kirchmeier[46], C. Kirfel[22], J. Kirk[138], A. E. Kiryunin[111], T. Kishimoto[158], D. P. Kisliuk[161], C. Kitsaki[9], O. Kivernyk[22], T. Klapdor-Kleingrothaus[50], M. Klassen[59a], C. Klein[32], L. Klein[171], M. H. Klein[102], M. Klein[88], U. Klein[88], P. Klimek[34], A. Klimentov[27], F. Klimpel[34], T. Klingl[22], T. Klioutchnikova[34], F. F. Klitzner[110], P. Kluit[115], S. Kluth[111], E. Kneringer[74], T. M. Knight[161], A. Knue[50], D. Kobayashi[85], M. Kobel[46], M. Kocian[148], T. Kodama[158], P. Kodys[137], D. M. Koeck[151], P. T. Koenig[22], T. Koffas[32], N. M. Köhler[34], M. Kolb[139], I. Koletsou[4], T. Komarek[125], K. Köneke[50], A. X. Y. Kong[1], T. Kono[121], V. Konstantinides[92], N. Konstantinidis[92], B. Konya[94], R. Kopeliansky[63], S. Koperny[81a], K. Korcyl[82], K. Kordas[157], G. Koren[156], A. Korn[92], S. Korn[51], I. Korolkov[12], E. V. Korolkova[144], N. Korotkova[109], B. Kortman[115], O. Kortner[111], S. Kortner[111], W. H. Kostecka[116], V. V. Kostyukhin[144,160], A. Kotsokechagia[62], A. Kotwal[47], A. Koulouris[34], A. Kourkoumeli-Charalampidi[68a,68b], C. Kourkoumelis[8], E. Kourlitis[5], O. Kovanda[151], R. Kowalewski[170], W. Kozanecki[139], A. S. Kozhin[118], V. A. Kramarenko[109], G. Kramberger[89], P. Kramer[96], D. Krasnopevtsev[58a], M. W. Krasny[130], A. Krasznahorkay[34], J. A. Kremer[96], J. Kretzschmar[88], K. Kreul[17], P. Krieger[161], F. Krieter[110], S. Krishnamurthy[99], A. Krishnan[59b], M. Krivos[137], K. Krizka[16], K. Kroeninger[45], H. Kroha[111], J. Kroll[135], J. Kroll[131], K. S. Krowpman[103], U. Kruchonak[77], H. Krüger[22], N. Krumnack[76], M. C. Kruse[47], J. A. Krzysiak[82], A. Kubota[159], O. Kuchinskaia[160], S. Kuday[3a], D. Kuechler[44], J. T. Kuechler[44], S. Kuehn[34], T. Kuhl[44], V. Kukhtin[77], Y. Kulchitsky[104,ad], S. Kuleshov[141b], M. Kumar[31f], N. Kumari[98], M. Kuna[56], A. Kupco[135], T. Kupfer[45], O. Kuprash[50], H. Kurashige[80], L. L. Kurchaninov[162a], Y. A. Kurochkin[104], A. Kurova[108], M. G. Kurth[13a,13d], E. S. Kuwertz[34], M. Kuze[159], A. K. Kvam[143], J. Kvita[125], T. Kwan[100], K. W. Kwok[60a], C. Lacasta[168], F. Lacava[70a,70b], H. Lacker[17], D. Lacour[130], N. N. Lad[92], E. Ladygin[77], R. Lafaye[4], B. Laforge[130], T. Lagouri[141c], S. Lai[51], I. K. Lakomiec[81a], N. Lalloue[56], J. E. Lambert[123], S. Lammers[63], W. Lampl[6], C. Lampoudis[157], E. Lançon[27], U. Landgraf[50], M. P. J. Landon[90], V. S. Lang[50], J. C. Lange[51], R. J. Langenberg[99], A. J. Lankford[165], F. Lanni[27], K. Lantzsch[22], A. Lanza[68a], A. Lapertosa[53a,53b], J. F. Laporte[139], T. Lari[66a], F. Lasagni Manghi[21b], M. Lassnig[34], V. Latonova[135], T. S. Lau[60a], A. Laudrain[96], A. Laurier[32], M. Lavorgna[67a,67b], S. D. Lawlor[91], Z. Lawrence[97], M. Lazzaroni[66a,66b], B. Le[97], B. Leban[89], A. Lebedev[76], M. LeBlanc[34], T. LeCompte[5], F. Ledroit-Guillon[56], A. C. A. Lee[92], G. R. Lee[15], L. Lee[57], S. C. Lee[153], S. Lee[76], L. L. Leeuw[31c], B. Lefebvre[162a], H. P. Lefebvre[91], M. Lefebvre[170], C. Leggett[16], K. Lehmann[147], N. Lehmann[18], G. Lehmann Miotto[34], W. A. Leight[44], A. Leisos[157,u], M. A. L. Leite[78c], C. E. Leitgeb[44], R. Leitner[137], K. J. C. Leney[40], T. Lenz[22], S. Leone[69a], C. Leonidopoulos[48], A. Leopold[130], C. Leroy[106], R. Les[103], C. G. Lester[30], M. Levchenko[132], J. Levêque[4], D. Levin[102], L. J. Levinson[174], D. J. Lewis[19], B. Li[13b], B. Li[58b], C. Li[58a], C-Q. Li[58c,58d], H. Li[58a], H. Li[58b], H. Li[58b], J. Li[58c], K. Li[143], L. Li[58c], M. Li[13a,13d], Q. Y. Li[58a], S. Li[58c,58d,c], T. Li[58b], X. Li[44], Y. Li[44], Z. Li[58b], Z. Li[129], Z. Li[100], Z. Li[88], Z. Liang[13a], M. Liberatore[44], B. Liberti[71a], K. Lie[60c], J. Lieber Marin[78b], K. Lin[103], R. A. Linck[63], R. E. Lindley[6], J. H. Lindon[2], A. Linss[44], E. Lipeles[131], A. Lipniacka[15], T. M. Liss[167,ai], A. Lister[169], J. D. Little[7], B. Liu[13a], B. X. Liu[147], J. B. Liu[58a], J. K. K. Liu[35], K. Liu[58c,58d], M. Liu[58a], M. Y. Liu[58a], P. Liu[13a], X. Liu[58a], Y. Liu[44], Y. Liu[13c,13d], Y. L. Liu[102], Y. W. Liu[58a], M. Livan[68a,68b], A. Lleres[56], J. Llorente Merino[147], S. L. Lloyd[90], E. M. Lobodzinska[44], P. Loch[6], S. Loffredo[71a,71b], T. Lohse[17], K. Lohwasser[144], M. Lokajicek[135], J. D. Long[167], I. Longarini[70a,70b], L. Longo[34], R. Longo[167], I. Lopez Paz[12], A. Lopez Solis[44], J. Lorenz[110], N. Lorenzo Martinez[4], A. M. Lory[110], A. Lösle[50], X. Lou[43a,43b], X. Lou[13a], A. Lounis[62], J. Love[5], P. A. Love[87], J. J. Lozano Bahilo[168], G. Lu[13a], M. Lu[58a], S. Lu[131], Y. J. Lu[61], H. J. Lubatti[143], C. Luci[70a,70b], F. L. Lucio Alves[13c], A. Lucotte[56],

F. Luehring[63], I. Luise[150], L. Luminari[70a], O. Lundberg[149], B. Lund-Jensen[149], N. A. Luongo[126], M. S. Lutz[156], D. Lynn[27], H. Lyons[88], R. Lysak[135], E. Lytken[94], F. Lyu[13a], V. Lyubushkin[77], T. Lyubushkina[77], H. Ma[27], L. L. Ma[58b], Y. Ma[92], D. M. Mac Donell[170], G. Maccarrone[49], C. M. Macdonald[144], J. C. MacDonald[144], R. Madar[36], W. F. Mader[46], M. Madugoda Ralalage Don[124], N. Madysa[46], J. Maeda[80], T. Maeno[27], M. Maerker[46], V. Magerl[50], J. Magro[64a,64c], D. J. Mahon[37], C. Maidantchik[78b], A. Maio[134a,134b,134d], K. Maj[81a], O. Majersky[26a], S. Majewski[126], N. Makovec[62], V. Maksimovic[14], B. Malaescu[130], Pa. Malecki[82], V. P. Maleev[132], F. Malek[56], D. Malito[39a,39b], U. Mallik[75], C. Malone[30], S. Maltezos[9], S. Malyukov[77], J. Mamuzic[168], G. Mancini[49], J. P. Mandalia[90], I. Mandić[89], L. Manhaes de Andrade Filho[78a], I. M. Maniatis[157], M. Manisha[139], J. Manjarres Ramos[46], K. H. Mankinen[94], A. Mann[110], A. Manousos[74], B. Mansoulie[139], I. Manthos[157], S. Manzoni[115], A. Marantis[157,u], G. Marchiori[130], M. Marcisovsky[135], L. Marcoccia[71a,71b], C. Marcon[94], M. Marjanovic[123], Z. Marshall[16], S. Marti-Garcia[168], T. A. Martin[172], V. J. Martin[48], B. Martin dit Latour[15], L. Martinelli[70a,70b], M. Martinez[12,v], P. Martinez Agullo[168], V. I. Martinez Outschoorn[99], S. Martin-Haugh[138], V. S. Martoiu[25b], A. C. Martyniuk[92], A. Marzin[34], S. R. Maschek[111], L. Masetti[96], T. Mashimo[158], J. Masik[97], A. L. Maslennikov[117a,117b], L. Massa[21b], P. Massarotti[67a,67b], P. Mastrandrea[69a,69b], A. Mastroberardino[39a,39b], T. Masubuchi[158], D. Matakias[27], T. Mathisen[166], A. Matic[110], N. Matsuzawa[158], J. Maurer[25b], B. Maček[89], D. A. Maximov[117a,117b], R. Mazini[153], I. Maznas[157], S. M. Mazza[140], C. Mc Ginn[27], J. P. Mc Gowan[100], S. P. Mc Kee[102], T. G. McCarthy[111], W. P. McCormack[16], E. F. McDonald[101], A. E. McDougall[115], J. A. Mcfayden[151], G. Mchedlidze[154b], M. A. McKay[40], K. D. McLean[170], S. J. McMahon[138], P. C. McNamara[101], R. A. McPherson[170,y], J. E. Mdhluli[31f], Z. A. Meadows[99], S. Meehan[34], T. Megy[36], S. Mehlhase[110], A. Mehta[88], B. Meirose[41], D. Melini[155], B. R. Mellado Garcia[31f], A. H. Melo[51], F. Meloni[44], A. Melzer[22], E. D. Mendes Gouveia[134a], A. M. Mendes Jacques Da Costa[19], H. Y. Meng[161], L. Meng[34], S. Menke[111], M. Mentink[34], E. Meoni[39a,39b], C. Merlassino[129], P. Mermod[52,*], L. Merola[67a,67b], C. Meroni[66a], G. Merz[102], O. Meshkov[107,109], J. K. R. Meshreki[146], J. Metcalfe[5], A. S. Mete[5], C. Meyer[63], J-P. Meyer[139], M. Michetti[17], R. P. Middleton[138], L. Mijović[48], G. Mikenberg[174], M. Mikestikova[135], M. Mikuž[89], H. Mildner[144], A. Milic[161], C. D. Milke[40], D. W. Miller[35], L. S. Miller[32], A. Milov[174], D. A. Milstead[43a,43b], T. Min[13c], A. A. Minaenko[118], I. A. Minashvili[154b], L. Mince[55], A. I. Mincer[120], B. Mindur[81a], M. Mineev[77], Y. Minegishi[158], Y. Mino[83], L. M. Mir[12], M. Miralles Lopez[168], M. Mironova[129], T. Mitani[173], V. A. Mitsou[168], M. Mittal[58c], O. Miu[161], P. S. Miyagawa[90], Y. Miyazaki[85], A. Mizukami[79], J. U. Mjörnmark[94], T. Mkrtchyan[59a], M. Mlynarikova[116], T. Moa[43a,43b], S. Mobius[51], K. Mochizuki[106], P. Moder[44], P. Mogg[110], A. F. Mohammed[13a], S. Mohapatra[37], G. Mokgatitswane[31f], B. Mondal[146], S. Mondal[136], K. Mönig[44], E. Monnier[98], L. Monsonis Romero[168], A. Montalbano[147], J. Montejo Berlingen[34], M. Montella[122], F. Monticelli[86], N. Morange[62], A. L. Moreira De Carvalho[134a], M. Moreno Llácer[168], C. Moreno Martinez[12], P. Morettini[53b], S. Morgenstern[172], D. Mori[147], M. Morii[57], M. Morinaga[158], V. Morisbak[128], A. K. Morley[34], A. P. Morris[92], L. Morvaj[34], P. Moschovakos[34], B. Moser[115], M. Mosidze[154b], T. Moskalets[50], P. Moskvitina[114], J. Moss[29,n], E. J. W. Moyse[99], S. Muanza[98], J. Mueller[133], R. Mueller[18], D. Muenstermann[87], G. A. Mullier[94], J. J. Mullin[131], D. P. Mungo[66a,66b], J. L. Munoz Martinez[12], F. J. Munoz Sanchez[97], M. Murin[97], P. Murin[26b], W. J. Murray[138,172], A. Murrone[66a,66b], J. M. Muse[123], M. Muškinja[16], C. Mwewa[27], A. G. Myagkov[118,ae], A. J. Myers[7], A. A. Myers[133], G. Myers[63], M. Myska[136], B. P. Nachman[16], O. Nackenhorst[45], A.Nag Nag[46], K. Nagai[129], K. Nagano[79], J. L. Nagle[27], E. Nagy[98], A. M. Nairz[34], Y. Nakahama[112], K. Nakamura[79], H. Nanjo[127], F. Napolitano[59a], R. Narayan[40], E. A. Narayanan[113], I. Naryshkin[132], M. Naseri[32], C. Nass[22], T. Naumann[44], G. Navarro[20a], J. Navarro-Gonzalez[168], R. Nayak[156], P. Y. Nechaeva[107], F. Nechansky[44], T. J. Neep[19], A. Negri[68a,68b], M. Negrini[21b], C. Nellist[114], C. Nelson[100], K. Nelson[102], S. Nemecek[135], M. Nessi[34,f], M. S. Neubauer[167], F. Neuhaus[96], J. Neundorf[44], R. Newhouse[169], P. R. Newman[19], C. W. Ng[133], Y. S. Ng[17], Y. W. Y. Ng[165], B. Ngair[33e], H. D. N. Nguyen[106], R. B. Nickerson[129], R. Nicolaidou[139], D. S. Nielsen[38], J. Nielsen[140], M. Niemeyer[51], N. Nikiforou[10], V. Nikolaenko[118,ae], I. Nikolic-Audit[130], K. Nikolopoulos[19], P. Nilsson[27], H. R. Nindhito[52], A. Nisati[70a], N. Nishu[2], R. Nisius[111], T. Nitta[173], T. Nobe[158], D. L. Noel[30], Y. Noguchi[83], I. Nomidis[130], M. A. Nomura[27], M. B. Norfolk[144], R. R. B. Norisam[92], J. Novak[89], T. Novak[44], O. Novgorodova[46], L. Novotny[136], R. Novotny[113], L. Nozka[125], K. Ntekas[165], E. Nurse[92], F. G. Oakham[32,aj], J. Ocariz[130], A. Ochi[80], I. Ochoa[134a], J. P. Ochoa-Ricoux[141a], S. Oda[85], S. Odaka[79], S. Oerdek[166], A. Ogrodnik[81a], A. Oh[97], C. C. Ohm[149], H. Oide[159], R. Oishi[158], M. L. Ojeda[44], Y. Okazaki[83], M. W. O'Keefe[88], Y. Okumura[158], A. Olariu[25b], L. F. Oleiro Seabra[134a],

S. A. Olivares Pino[141c], D. Oliveira Damazio[27], D. Oliveira Goncalves[78a], J. L. Oliver[165], M. J. R. Olsson[165], A. Olszewski[82], J. Olszowska[82], Ö.O. Öncel[22], D. C. O'Neil[147], A. P. O'neill[129], A. Onofre[134a,134e], P. U. E. Onyisi[10], R. G. Oreamuno Madriz[116], M. J. Oreglia[35], G. E. Orellana[86], D. Orestano[72a,72b], N. Orlando[12], R. S. Orr[161], V. O'Shea[55], R. Ospanov[58a], G. Otero y Garzon[28], H. Otono[85], P. S. Ott[59a], G. J. Ottino[16], M. Ouchrif[33d], J. Ouellette[27], F. Ould-Saada[128], A. Ouraou[139,*], Q. Ouyang[13a], M. Owen[55], R. E. Owen[138], K. Y. Oyulmaz[11c], V. E. Ozcan[11c], N. Ozturk[7], S. Ozturk[11c], J. Pacalt[125], H. A. Pacey[30], K. Pachal[47], A. Pacheco Pages[12], C. Padilla Aranda[12], S. Pagan Griso[16], G. Palacino[63], S. Palazzo[48], S. Palestini[34], M. Palka[81b], P. Palni[81a], D. K. Panchal[10], C. E. Pandini[52], J. G. Panduro Vazquez[91], P. Pani[44], G. Panizzo[64a,64c], L. Paolozzi[52], C. Papadatos[106], S. Parajuli[40], A. Paramonov[5], C. Paraskevopoulos[9], D. Paredes Hernandez[60b], S. R. Paredes Saenz[129], B. Parida[174], T. H. Park[161], A. J. Parker[29], M. A. Parker[30], F. Parodi[53a,53b], E. W. Parrish[116], J. A. Parsons[37], U. Parzefall[50], L. Pascual Dominguez[156], V. R. Pascuzzi[16], F. Pasquali[115], E. Pasqualucci[70a], S. Passaggio[53b], F. Pastore[91], P. Pasuwan[43a,43b], J. R. Pater[97], A. Pathak[175], J. Patton[88], T. Pauly[34], J. Pearkes[148], M. Pedersen[128], L. Pedraza Diaz[114], R. Pedro[134a], T. Peiffer[51], S. V. Peleganchuk[117a,117b], O. Penc[135], C. Peng[60b], H. Peng[58a], M. Penzin[160], B. S. Peralva[78a], A. P. Pereira Peixoto[134a], L. Pereira Sanchez[43a,43b], D. V. Perepelitsa[27], E. Perez Codina[162a], M. Perganti[9], L. Perini[66a,66b], H. Pernegger[34], S. Perrella[34], A. Perrevoort[115], K. Peters[44], R. F. Y. Peters[97], B. A. Petersen[34], T. C. Petersen[38], E. Petit[98], V. Petousis[136], C. Petridou[157], P. Petroff[62], F. Petrucci[72a,72b], A. Petrukhin[146], M. Pettee[177], N. E. Pettersson[34], K. Petukhova[137], A. Peyaud[139], R. Pezoa[141d], L. Pezzotti[34], G. Pezzullo[177], T. Pham[101], P. W. Phillips[138], M. W. Phipps[167], G. Piacquadio[150], E. Pianori[16], F. Piazza[66a,66b], A. Picazio[99], R. Piegaia[28], D. Pietreanu[25b], J. E. Pilcher[35], A. D. Pilkington[97], M. Pinamonti[64a,64c], J. L. Pinfold[2], C. Pitman Donaldson[92], D. A. Pizzi[32], L. Pizzimento[71a,71b], A. Pizzini[115], M.-A. Pleier[27], V. Plesanovs[50], V. Pleskot[137], E. Plotnikova[77], P. Podberezko[117a,117b], R. Poettgen[94], R. Poggi[52], L. Poggioli[130], I. Pogrebnyak[103], D. Pohl[22], I. Pokharel[51], G. Polesello[68a], A. Poley[147,162a], A. Policicchio[70a,70b], R. Polifka[137], A. Polini[21b], C. S. Pollard[129], Z. B. Pollock[122], V. Polychronakos[27], D. Ponomarenko[108], L. Pontecorvo[34], S. Popa[25a], G. A. Popeneciu[25d], L. Portales[4], D. M. Portillo Quintero[162a], S. Pospisil[136], P. Postolache[25c], K. Potamianos[129], I. N. Potrap[77], C. J. Potter[30], H. Potti[1], T. Poulsen[44], J. Poveda[168], T. D. Powell[144], G. Pownall[44], M. E. Pozo Astigarraga[34], A. Prades Ibanez[168], P. Pralavorio[98], M. M. Prapa[42], S. Prell[76], D. Price[97], M. Primavera[65a], M. A. Principe Martin[95], M. L. Proffitt[143], N. Proklova[108], K. Prokofiev[60c], F. Prokoshin[77], S. Protopopescu[27], J. Proudfoot[5], M. Przybycien[81a], D. Pudzha[132], P. Puzo[62], D. Pyatiizbyantseva[108], J. Qian[102], Y. Qin[97], T. Qiu[90], A. Quadt[51], M. Queitsch-Maitland[34], G. Rabanal Bolanos[57], F. Ragusa[66a,66b], J. A. Raine[52], S. Rajagopalan[27], K. Ran[13a,13d], D. F. Rassloff[59a], D. M. Rauch[44], S. Rave[96], B. Ravina[55], I. Ravinovich[174], M. Raymond[34], A. L. Read[128], N. P. Readioff[144], D. M. Rebuzzi[68a,68b], G. Redlinger[27], K. Reeves[41], D. Reikher[156], A. Reiss[96], A. Rej[146], C. Rembser[34], A. Renardi[44], M. Renda[25b], M. B. Rendel[111], A. G. Rennie[55], S. Resconi[66a], M. Ressegotti[53a,53b], E. D. Resseguie[16], S. Rettie[92], B. Reynolds[122], E. Reynolds[19], M. Rezaei Estabragh[176], O. L. Rezanova[117a,117b], P. Reznicek[137], E. Ricci[73a,73b], R. Richter[111], S. Richter[44], E. Richter-Was[81b], M. Ridel[130], P. Rieck[111], P. Riedler[34], O. Rifki[44], M. Rijssenbeek[150], A. Rimoldi[68a,68b], M. Rimoldi[44], L. Rinaldi[21a,21b], T. T. Rinn[167], M. P. Rinnagel[110], G. Ripellino[149], I. Riu[12], P. Rivadeneira[44], J. C. Rivera Vergara[170], F. Rizatdinova[124], E. Rizvi[90], C. Rizzi[52], B. A. Roberts[172], S. H. Robertson[100,y], M. Robin[44], D. Robinson[30], C. M. Robles Gajardo[141d], M. Robles Manzano[96], A. Robson[55], A. Rocchi[71a,71b], C. Roda[69a,69b], S. Rodriguez Bosca[59a], A. Rodriguez Rodriguez[50], A. M. Rodríguez Vera[162b], S. Roe[34], A. R. Roepe[123], J. Roggel[176], O. Røhne[128], R. A. Rojas[141d], B. Roland[50], C. P. A. Roland[63], J. Roloff[27], A. Romaniouk[108], M. Romano[21b], A. C. Romero Hernandez[167], N. Rompotis[88], M. Ronzani[120], L. Roos[130], S. Rosati[70a], B. J. Rosser[131], E. Rossi[161], E. Rossi[4], E. Rossi[67a,67b], L. P. Rossi[53b], L. Rossini[44], R. Rosten[122], M. Rotaru[25b], B. Rottler[50], D. Rousseau[62], D. Rousso[30], G. Rovelli[68a,68b], A. Roy[10], A. Rozanov[98], Y. Rozen[155], X. Ruan[31f], A. J. Ruby[88], T. A. Ruggeri[1], F. Rühr[50], A. Ruiz-Martinez[168], A. Rummler[34], Z. Rurikova[50], N. A. Rusakovich[77], H. L. Russell[34], L. Rustige[36], J. P. Rutherfoord[6], E. M. Rüttinger[144], M. Rybar[137], E. B. Rye[128], A. Ryzhov[118], J. A. Sabater Iglesias[44], P. Sabatini[168], L. Sabetta[70a,70b], H.F-W. Sadrozinski[140], R. Sadykov[77], F. Safai Tehrani[70a], B. Safarzadeh Samani[151], M. Safdari[148], P. Saha[116], S. Saha[100], M. Sahinsoy[111], A. Sahu[176], M. Saimpert[139], M. Saito[158], T. Saito[158], D. Salamani[34], G. Salamanna[72a,72b], A. Salnikov[148], J. Salt[168], A. Salvador Salas[12], D. Salvatore[39a,39b], F. Salvatore[151], A. Salzburger[34], D. Sammel[50], D. Sampsonidis[157], D. Sampsonidou[58c,58d], J. Sánchez[168],

A. Sanchez Pineda[4], V. Sanchez Sebastian[168], H. Sandaker[128], C. O. Sander[44], I. G. Sanderswood[87], J. A. Sandesara[99], M. Sandhoff[176], C. Sandoval[20b], D. P. C. Sankey[138], M. Sannino[53a,53b], A. Sansoni[49], C. Santoni[36], H. Santos[134a,134b], S. N. Santpur[16], A. Santra[174], K. A. Saoucha[144], A. Sapronov[77], J. G. Saraiva[134a,134d], J. Sardain[98], O. Sasaki[79], K. Sato[163], C. Sauer[59b], F. Sauerburger[50], E. Sauvan[4], P. Savard[161,aj], R. Sawada[158], C. Sawyer[138], L. Sawyer[93], I. Sayago Galvan[168], C. Sbarra[21b], A. Sbrizzi[64a,64c], T. Scanlon[92], J. Schaarschmidt[143], P. Schacht[111], D. Schaefer[35], U. Schäfer[96], A. C. Schaffer[62], D. Schaile[110], R. D. Schamberger[150], E. Schanet[110], C. Scharf[17], N. Scharmberg[97], V. A. Schegelsky[132], D. Scheirich[137], F. Schenck[17], M. Schernau[165], C. Schiavi[53a,53b], L. K. Schildgen[22], Z. M. Schillaci[24], E. J. Schioppa[65a,65b], M. Schioppa[39a,39b], B. Schlag[96], K. E. Schleicher[50], S. Schlenker[34], K. Schmieden[96], C. Schmitt[96], S. Schmitt[44], L. Schoeffel[139], A. Schoening[59b], P. G. Scholer[50], E. Schopf[129], M. Schott[96], J. Schovancova[34], S. Schramm[52], F. Schroeder[176], H-C. Schultz-Coulon[59a], M. Schumacher[50], B. A. Schumm[140], Ph. Schune[139], A. Schwartzman[148], T. A. Schwarz[102], Ph. Schwemling[139], R. Schwienhorst[103], A. Sciandra[140], G. Sciolla[24], F. Scuri[69a], F. Scutti[101], C. D. Sebastiani[88], K. Sedlaczek[45], P. Seema[17], S. C. Seidel[113], A. Seiden[140], B. D. Seidlitz[27], T. Seiss[35], C. Seitz[44], J. M. Seixas[78b], G. Sekhniaidze[67a], S. J. Sekula[40], L. Selem[4], N. Semprini-Cesari[21a,21b], S. Sen[47], C. Serfon[27], L. Serin[62], L. Serkin[64a,64b], M. Sessa[72a,72b], H. Severini[123], S. Sevova[148], F. Sforza[53a,53b], A. Sfyrla[52], E. Shabalina[51], R. Shaheen[149], J. D. Shahinian[131], N. W. Shaikh[43a,43b], D. Shaked Renous[174], L. Y. Shan[13a], M. Shapiro[16], A. Sharma[34], A. S. Sharma[1], S. Sharma[44], P. B. Shatalov[119], K. Shaw[151], S. M. Shaw[97], P. Sherwood[92], L. Shi[92], C. O. Shimmin[177], Y. Shimogama[173], J. D. Shinner[91], I. P. J. Shipsey[129], S. Shirabe[52], M. Shiyakova[77], J. Shlomi[174], M. J. Shochet[35], J. Shojaii[101], D. R. Shope[149], S. Shrestha[122], E. M. Shrif[31f], M. J. Shroff[170], E. Shulga[174], P. Sicho[135], A. M. Sickles[167], E. Sideras Haddad[31f], O. Sidiropoulou[34], A. Sidoti[21b], F. Siegert[46], Dj. Sijacki[14], J. M. Silva[19], M. V. Silva Oliveira[34], S. B. Silverstein[43a], S. Simion[62], R. Simoniello[34], N. D. Simpson[94], S. Simsek[11b], P. Sinervo[161], V. Sinetckii[109], S. Singh[147], S. Singh[161], S. Sinha[44], S. Sinha[31f], M. Sioli[21a,21b], I. Siral[126], S. Yu. Sivoklokov[109], J. Sjölin[43a,43b], A. Skaf[51], E. Skorda[94], P. Skubic[123], M. Slawinska[82], K. Sliwa[164], V. Smakhtin[174], B. H. Smart[138], J. Smiesko[137], S. Yu. Smirnov[108], Y. Smirnov[108], L. N. Smirnova[109,r], O. Smirnova[94], E. A. Smith[35], H. A. Smith[129], M. Smizanska[87], K. Smolek[136], A. Smykiewicz[82], A. A. Snesarev[107], H. L. Snoek[115], S. Snyder[27], R. Sobie[170,y], A. Soffer[156], F. Sohns[51], C. A. Solans Sanchez[34], E. Yu. Soldatov[108], U. Soldevila[168], A. A. Solodkov[118], S. Solomon[50], A. Soloshenko[77], O. V. Solovyanov[118], V. Solovyev[132], P. Sommer[144], H. Son[164], A. Sonay[12], W. Y. Song[162b], A. Sopczak[136], A. L. Sopio[92], F. Sopkova[26b], S. Sottocornola[68a,68b], R. Soualah[64a,64c], A. M. Soukharev[117a,117b], Z. Soumaimi[33e], D. South[44], S. Spagnolo[65a,65b], M. Spalla[111], M. Spangenberg[172], F. Spanò[91], D. Sperlich[50], T. M. Spieker[59a], G. Spigo[34], M. Spina[151], D. P. Spiteri[55], M. Spousta[137], A. Stabile[66a,66b], B. L. Stamas[116], R. Stamen[59a], M. Stamenkovic[115], A. Stampekis[19], M. Standke[22], E. Stanecka[82], B. Stanislaus[34], M. M. Stanitzki[44], M. Stankaityte[129], B. Stapf[44], E. A. Starchenko[118], G. H. Stark[140], J. Stark[98], D. M. Starko[162b], P. Staroba[135], P. Starovoitov[59a], S. Stärz[100], R. Staszewski[82], G. Stavropoulos[42], P. Steinberg[27], A. L. Steinhebel[126], B. Stelzer[147,162a], H. J. Stelzer[133], O. Stelzer-Chilton[162a], H. Stenzel[54], T. J. Stevenson[151], G. A. Stewart[34], M. C. Stockton[34], G. Stoicea[25b], M. Stolarski[134a], S. Stonjek[111], A. Straessner[46], J. Strandberg[149], S. Strandberg[43a,43b], M. Strauss[123], T. Strebler[98], P. Strizenec[26b], R. Ströhmer[171], D. M. Strom[126], L. R. Strom[44], R. Stroynowski[40], A. Strubig[43a,43b], S. A. Stucci[27], B. Stugu[15], J. Stupak[123], N. A. Styles[44], D. Su[148], S. Su[58a], W. Su[58c,58d,143], X. Su[58a], K. Sugizaki[158], V. V. Sulin[107], M. J. Sullivan[88], D. M. S. Sultan[52], L. Sultanaliyeva[107], S. Sultansoy[3c], T. Sumida[83], S. Sun[102], S. Sun[175], X. Sun[97], O. Sunneborn Gudnadottir[166], C. J. E. Suster[152], M. R. Sutton[151], M. Svatos[135], M. Swiatlowski[162a], T. Swirski[171], I. Sykora[26a], M. Sykora[137], T. Sykora[137], D. Ta[96], K. Tackmann[44,w], A. Taffard[165], R. Tafirout[162a], R. H. M. Taibah[130], R. Takashima[84], K. Takeda[80], T. Takeshita[145], E. P. Takeva[48], Y. Takubo[79], M. Talby[98], A. A. Talyshev[117a,117b], K. C. Tam[60b], N. M. Tamir[156], A. Tanaka[158], J. Tanaka[158], R. Tanaka[62], J. Tang[58c], Z. Tao[169], S. Tapia Araya[76], S. Tapprogge[96], A. Tarek Abouelfadl Mohamed[103], S. Tarem[155], K. Tariq[58b], G. Tarna[25b], G. F. Tartarelli[66a], P. Tas[137], M. Tasevsky[135], E. Tassi[39a,39b], G. Tateno[158], Y. Tayalati[33e], G. N. Taylor[101], W. Taylor[162b], H. Teagle[88], A. S. Tee[175], R. Teixeira De Lima[148], P. Teixeira-Dias[91], H. Ten Kate[34], J. J. Teoh[115], K. Terashi[158], J. Terron[95], S. Terzo[12], M. Testa[49], R. J. Teuscher[161,y], N. Themistokleous[48], T. Theveneaux-Pelzer[17], O. Thielmann[176], D. W. Thomas[91], J. P. Thomas[19], E. A. Thompson[44], P. D. Thompson[19], E. Thomson[131], E. J. Thorpe[90], Y. Tian[51], V. O. Tikhomirov[107,af], Yu. A. Tikhonov[117a,117b], S. Timoshenko[108], P. Tipton[177], S. Tisserant[98], S. H. Tlou[31f],

A. Tnourji[36], K. Todome[21a,21b], S. Todorova-Nova[137], S. Todt[46], M. Togawa[79], J. Tojo[85], S. Tokár[26a], K. Tokushuku[79], E. Tolley[122], R. Tombs[30], M. Tomoto[79,112], L. Tompkins[148], P. Tornambe[99], E. Torrence[126], H. Torres[46], E. Torró Pastor[168], M. Toscani[28], C. Tosciri[35], J. Toth[98,x], D. R. Tovey[144], A. Traeet[15], C. J. Treado[120], T. Trefzger[171], A. Tricoli[27], I. M. Trigger[162a], S. Trincaz-Duvoid[130], D. A. Trischuk[169], W. Trischuk[161], B. Trocmé[56], A. Trofymov[62], C. Troncon[66a], F. Trovato[151], L. Truong[31c], M. Trzebinski[82], A. Trzupek[82], F. Tsai[150], A. Tsiamis[157], P. V. Tsiareshka[104,ad], A. Tsirigotis[157,u], V. Tsiskaridze[150], E. G. Tskhadadze[154a], M. Tsopoulou[157], I. I. Tsukerman[119], V. Tsulaia[16], S. Tsuno[79], O. Tsur[155], D. Tsybychev[150], Y. Tu[60b], A. Tudorache[25b], V. Tudorache[25b], A. N. Tuna[34], S. Turchikhin[77], I. Turk Cakir[3a], R. J. Turner[19], R. Turra[66a], P. M. Tuts[37], S. Tzamarias[157], P. Tzanis[9], E. Tzovara[96], K. Uchida[158], F. Ukegawa[163], G. Unal[34], M. Unal[10], A. Undrus[27], G. Unel[165], F. C. Ungaro[101], K. Uno[158], J. Urban[26b], P. Urquijo[101], G. Usai[7], R. Ushioda[159], M. Usman[106], Z. Uysal[11d], V. Vacek[136], B. Vachon[100], K. O. H. Vadla[128], T. Vafeiadis[34], C. Valderanis[110], E. Valdes Santurio[43a,43b], M. Valente[162a], S. Valentinetti[21a,21b], A. Valero[168], L. Valéry[44], R. A. Vallance[19], A. Vallier[98], J. A. Valls Ferrer[168], T. R. Van Daalen[143], P. Van Gemmeren[5], S. Van Stroud[92], I. Van Vulpen[115], M. Vanadia[71a,71b], W. Vandelli[34], M. Vandenbroucke[139], E. R. Vandewall[124], D. Vannicola[156], L. Vannoli[53a,53b], R. Vari[70a], E. W. Varnes[6], C. Varni[16], T. Varol[153], D. Varouchas[62], K. E. Varvell[152], M. E. Vasile[25b], L. Vaslin[36], G. A. Vasquez[170], F. Vazeille[36], D. Vazquez Furelos[12], T. Vazquez Schroeder[34], J. Veatch[51], V. Vecchio[97], M. J. Veen[115], I. Veliscek[129], L. M. Veloce[161], F. Veloso[134a,134c], S. Veneziano[70a], A. Ventura[65a,65b], A. Verbytskyi[111], M. Verducci[69a,69b], C. Vergis[22], M. Verissimo De Araujo[78b], W. Verkerke[115], A. T. Vermeulen[115], J. C. Vermeulen[115], C. Vernieri[148], P. J. Verschuuren[91], M. Vessella[99], M. L. Vesterbacka[120], M. C. Vetterli[147,aj], A. Vgenopoulos[157], N. Viaux Maira[141d], T. Vickey[144], O. E. Vickey Boeriu[144], G. H. A. Viehhauser[129], L. Vigani[59b], M. Villa[21a,21b], M. Villaplana Perez[168], E. M. Villhauer[48], E. Vilucchi[49], M. G. Vincter[32], G. S. Virdee[19], A. Vishwakarma[48], C. Vittori[21a,21b], I. Vivarelli[151], V. Vladimirov[172], E. Voevodina[111], M. Vogel[176], P. Vokac[136], J. Von Ahnen[44], E. Von Toerne[22], V. Vorobel[137], K. Vorobev[108], M. Vos[168], J. H. Vossebeld[88], M. Vozak[97], L. Vozdecky[90], N. Vranjes[14], M. Vranjes Milosavljevic[14], V. Vrba[136,*], M. Vreeswijk[115], N. K. Vu[98], R. Vuillermet[34], O. V. Vujinovic[96], I. Vukotic[35], S. Wada[163], C. Wagner[99], W. Wagner[176], S. Wahdan[176], H. Wahlberg[86], R. Wakasa[163], M. Wakida[112], V. M. Walbrecht[111], J. Walder[138], R. Walker[110], S. D. Walker[91], W. Walkowiak[146], A. M. Wang[57], A. Z. Wang[175], C. Wang[58a], C. Wang[58c], H. Wang[16], J. Wang[60a], P. Wang[40], R.-J. Wang[96], R. Wang[57], R. Wang[116], S. M. Wang[153], S. Wang[58b], T. Wang[58a], W. T. Wang[75], W. X. Wang[58a], X. Wang[13c], X. Wang[167], X. Wang[58c], Y. Wang[58a], Z. Wang[102], C. Wanotayaroj[34], A. Warburton[100], C. P. Ward[30], R. J. Ward[19], N. Warrack[55], A. T. Watson[19], M. F. Watson[19], G. Watts[143], B. M. Waugh[92], A. F. Webb[10], C. Weber[27], M. S. Weber[18], S. A. Weber[32], S. M. Weber[59a], C. Wei[58a], Y. Wei[129], A. R. Weidberg[129], J. Weingarten[45], M. Weirich[96], C. Weiser[50], T. Wenaus[27], B. Wendland[45], T. Wengler[34], S. Wenig[34], N. Wermes[22], M. Wessels[59a], K. Whalen[126], A. M. Wharton[87], A. S. White[57], A. White[7], M. J. White[1], D. Whiteson[165], L. Wickremasinghe[127], W. Wiedenmann[175], C. Wiel[46], M. Wielers[138], N. Wieseotte[96], C. Wiglesworth[38], L. A. M. Wiik-Fuchs[50], D. J. Wilbern[123], H. G. Wilkens[34], L. J. Wilkins[91], D. M. Williams[37], H. H. Williams[131], S. Williams[30], S. Willocq[99], P. J. Windischhofer[129], I. Wingerter-Seez[4], F. Winklmeier[126], B. T. Winter[50], M. Wittgen[148], M. Wobisch[93], A. Wolf[96], R. Wölker[129], J. Wollrath[165], M. W. Wolter[82], H. Wolters[134a,134c], V. W. S. Wong[169], A. F. Wongel[44], S. D. Worm[44], B. K. Wosiek[82], K. W. Woźniak[82], K. Wraight[55], J. Wu[13a,13d], S. L. Wu[175], X. Wu[52], Y. Wu[58a], Z. Wu[58a,139], J. Wuerzinger[129], T. R. Wyatt[97], B. M. Wynne[48], S. Xella[38], L. Xia[13c], M. Xia[13b], J. Xiang[60c], X. Xiao[102], M. Xie[58a], X. Xie[58a], I. Xiotidis[151], D. Xu[13a], H. Xu[58a], H. Xu[58a], L. Xu[58a], R. Xu[131], T. Xu[58a], W. Xu[102], Y. Xu[13b], Z. Xu[58b], Z. Xu[148], B. Yabsley[152], S. Yacoob[31a], N. Yamaguchi[85], Y. Yamaguchi[159], M. Yamatani[158], H. Yamauchi[163], T. Yamazaki[16], Y. Yamazaki[80], J. Yan[58c], S. Yan[129], Z. Yan[23], H. J. Yang[58c,58d], H. T. Yang[16], S. Yang[58a], T. Yang[60c], X. Yang[58a], X. Yang[13a], Y. Yang[158], Z. Yang[58a,102], W-M. Yao[16], Y. C. Yap[44], H. Ye[13c], J. Ye[40], S. Ye[27], I. Yeletskikh[77], M. R. Yexley[87], P. Yin[37], K. Yorita[173], K. Yoshihara[76], C. J. S. Young[50], C. Young[148], R. Yuan[58b,i], X. Yue[59a], M. Zaazoua[33e], B. Zabinski[82], G. Zacharis[9], E. Zaid[48], A. M. Zaitsev[118,ae], T. Zakareishvili[154b], N. Zakharchuk[32], S. Zambito[34], D. Zanzi[50], S. V. Zeißner[45], C. Zeitnitz[176], J. C. Zeng[167], D. T. Zenger Jr[24], O. Zenin[118], T. Ženiš[26a], S. Zenz[90], S. Zerradi[33a], D. Zerwas[62], B. Zhang[13c], D. F. Zhang[13b], G. Zhang[13b], J. Zhang[5], K. Zhang[13a], L. Zhang[13c], M. Zhang[167], R. Zhang[175], S. Zhang[102], X. Zhang[58c], X. Zhang[58b], Z. Zhang[62], P. Zhao[47], Y. Zhao[140], Z. Zhao[58a], A. Zhemchugov[77], Z. Zheng[148], D. Zhong[167], B. Zhou[102], C. Zhou[175], H. Zhou[6], N. Zhou[58c], Y. Zhou[6], C. G. Zhu[58b], C. Zhu[13a,13d], H. L. Zhu[58a],

H. Zhu[13a], J. Zhu[102], Y. Zhu[58a], X. Zhuang[13a], K. Zhukov[107], V. Zhulanov[117a,117b], D. Zieminska[63], N. I. Zimine[77], S. Zimmermann[50,*], J. Zinsser[59b], M. Ziolkowski[146], L. Živković[14], A. Zoccoli[21a,21b], K. Zoch[52], T. G. Zorbas[144], O. Zormpa[42], W. Zou[37], L. Zwalinski[34]

[1] Department of Physics, University of Adelaide, Adelaide, Australia
[2] Department of Physics, University of Alberta, Edmonton, AB, Canada
[3] [(a)]Department of Physics, Ankara University, Ankara, Turkey; [(b)]Application and Research Center for Advanced Studies, Istanbul Aydin University, Istanbul, Turkey; [(c)]Division of Physics, TOBB University of Economics and Technology, Ankara, Turkey
[4] LAPP, Univ. Savoie Mont Blanc, CNRS/IN2P3, Annecy, France
[5] High Energy Physics Division, Argonne National Laboratory, Argonne, IL, USA
[6] Department of Physics, University of Arizona, Tucson, AZ, USA
[7] Department of Physics, University of Texas at Arlington, Arlington, TX, USA
[8] Physics Department, National and Kapodistrian University of Athens, Athens, Greece
[9] Physics Department, National Technical University of Athens, Zografou, Greece
[10] Department of Physics, University of Texas at Austin, Austin, TX, USA
[11] [(a)]Faculty of Engineering and Natural Sciences, Bahcesehir University, Istanbul, Turkey; [(b)]Faculty of Engineering and Natural Sciences, Istanbul Bilgi University, Istanbul, Turkey; [(c)]Department of Physics, Bogazici University, Istanbul, Turkey; [(d)]Department of Physics Engineering, Gaziantep University, Gaziantep, Turkey
[12] Institut de Física d'Altes Energies (IFAE), Barcelona Institute of Science and Technology, Barcelona, Spain
[13] [(a)]Institute of High Energy Physics, Chinese Academy of Sciences, Beijing, China; [(b)]Physics Department, Tsinghua University, Beijing, China; [(c)]Department of Physics, Nanjing University, Nanjing, China; [(d)]University of Chinese Academy of Science (UCAS), Beijing, China
[14] Institute of Physics, University of Belgrade, Belgrade, Serbia
[15] Department for Physics and Technology, University of Bergen, Bergen, Norway
[16] Physics Division, Lawrence Berkeley National Laboratory and University of California, Berkeley, CA, USA
[17] Institut für Physik, Humboldt Universität zu Berlin, Berlin, Germany
[18] Albert Einstein Center for Fundamental Physics and Laboratory for High Energy Physics, University of Bern, Bern, Switzerland
[19] School of Physics and Astronomy, University of Birmingham, Birmingham, UK
[20] [(a)]Facultad de Ciencias y Centro de Investigaciónes, Universidad Antonio Nariño, Bogotá, Colombia; [(b)]Departamento de Física, Universidad Nacional de Colombia, Bogotá, Colombia
[21] [(a)]Dipartimento di Fisica e Astronomia A. Righi, Università di Bologna, Bologna, Italy; [(b)]INFN Sezione di Bologna, Bologna, Italy
[22] Physikalisches Institut, Universität Bonn, Bonn, Germany
[23] Department of Physics, Boston University, Boston, MA, USA
[24] Department of Physics, Brandeis University, Waltham, MA, USA
[25] [(a)]Transilvania University of Brasov, Brasov, Romania; [(b)]Horia Hulubei National Institute of Physics and Nuclear Engineering, Bucharest, Romania; [(c)]Department of Physics, Alexandru Ioan Cuza University of Iasi, Iasi, Romania; [(d)]National Institute for Research and Development of Isotopic and Molecular Technologies, Physics Department, Cluj-Napoca, Romania; [(e)]University Politehnica Bucharest, Bucharest, Romania; [(f)]West University in Timisoara, Timisoara, Romania
[26] [(a)]Faculty of Mathematics, Physics and Informatics, Comenius University, Bratislava, Slovak Republic; [(b)]Department of Subnuclear Physics, Institute of Experimental Physics of the Slovak Academy of Sciences, Kosice, Slovak Republic
[27] Physics Department, Brookhaven National Laboratory, Upton, NY, USA
[28] Departamento de Física (FCEN) and IFIBA, Universidad de Buenos Aires and CONICET, Buenos Aires, Argentina
[29] California State University, Long Beach, CA, USA
[30] Cavendish Laboratory, University of Cambridge, Cambridge, UK
[31] [(a)]Department of Physics, University of Cape Town, Cape Town, South Africa; [(b)] iThemba Labs, Western Cape, South Africa; [(c)]Department of Mechanical Engineering Science, University of Johannesburg, Johannesburg, South Africa; [(d)]National Institute of Physics, University of the Philippines Diliman, Quezon City, Philippines; [(e)]Department of Physics, University of South Africa, Pretoria, South Africa; [(f)]School of Physics, University of the Witwatersrand, Johannesburg, South Africa

[32] Department of Physics, Carleton University, Ottawa, ON, Canada
[33] [(a)]Faculté des Sciences Ain Chock, Réseau Universitaire de Physique des Hautes Energies-Université Hassan II, Casablanca, Morocco; [(b)]Faculté des Sciences, Université Ibn-Tofail, Kenitra, Morocco; [(c)]Faculté des Sciences Semlalia, Université Cadi Ayyad, LPHEA-Marrakech, Marrakech, Morocco; [(d)]LPMR, Faculté des Sciences, Université Mohamed Premier, Oujda, Morocco; [(e)]Faculté des sciences, Université Mohammed V, Rabat, Morocco
[34] CERN, Geneva, Switzerland
[35] Enrico Fermi Institute, University of Chicago, Chicago, IL, USA
[36] LPC, Université Clermont Auvergne, CNRS/IN2P3, Clermont-Ferrand, France
[37] Nevis Laboratory, Columbia University, Irvington, NY, USA
[38] Niels Bohr Institute, University of Copenhagen, Copenhagen, Denmark
[39] [(a)]Dipartimento di Fisica, Università della Calabria, Rende, Italy; [(b)]INFN Gruppo Collegato di Cosenza, Laboratori Nazionali di Frascati, Frascati, Italy
[40] Physics Department, Southern Methodist University, Dallas, TX, USA
[41] Physics Department, University of Texas at Dallas, Richardson, TX, USA
[42] National Centre for Scientific Research "Demokritos", Agia Paraskevi, Greece
[43] [(a)]Department of Physics, Stockholm University, Stockholm, Sweden; [(b)]Oskar Klein Centre, Stockholm, Sweden
[44] Deutsches Elektronen-Synchrotron DESY, Hamburg and Zeuthen, Germany
[45] Fakultät Physik , Technische Universität Dortmund, Dortmund, Germany
[46] Institut für Kern- und Teilchenphysik, Technische Universität Dresden, Dresden, Germany
[47] Department of Physics, Duke University, Durham, NC, USA
[48] SUPA-School of Physics and Astronomy, University of Edinburgh, Edinburgh, UK
[49] INFN e Laboratori Nazionali di Frascati, Frascati, Italy
[50] Physikalisches Institut, Albert-Ludwigs-Universität Freiburg, Freiburg, Germany
[51] II. Physikalisches Institut, Georg-August-Universität Göttingen, Göttingen, Germany
[52] Département de Physique Nucléaire et Corpusculaire, Université de Genève, Geneva, Switzerland
[53] [(a)]Dipartimento di Fisica, Università di Genova, Genoa, Italy; [(b)]INFN Sezione di Genova, Genoa, Italy
[54] II. Physikalisches Institut, Justus-Liebig-Universität Giessen, Giessen, Germany
[55] SUPA-School of Physics and Astronomy, University of Glasgow, Glasgow, UK
[56] LPSC, Université Grenoble Alpes, CNRS/IN2P3, Grenoble INP, Grenoble, France
[57] Laboratory for Particle Physics and Cosmology, Harvard University, Cambridge, MA, USA
[58] [(a)]Department of Modern Physics and State Key Laboratory of Particle Detection and Electronics, University of Science and Technology of China, Hefei, China; [(b)]Institute of Frontier and Interdisciplinary Science and Key Laboratory of Particle Physics and Particle Irradiation (MOE), Shandong University, Qingdao, China; [(c)]Key Laboratory for Particle Astrophysics and Cosmology (MOE), SKLPPC, School of Physics and Astronomy, Shanghai Jiao Tong University, Shanghai, China; [(d)]Tsung-Dao Lee Institute, Shanghai, China
[59] [(a)]Kirchhoff-Institut für Physik, Ruprecht-Karls-Universität Heidelberg, Heidelberg, Germany; [(b)]Physikalisches Institut, Ruprecht-Karls-Universität Heidelberg, Heidelberg, Germany
[60] [(a)]Department of Physics, Chinese University of Hong Kong, Shatin, N.T., Hong Kong, China; [(b)]Department of Physics, University of Hong Kong, Hong Kong, China; [(c)]Department of Physics and Institute for Advanced Study, Hong Kong University of Science and Technology, Clear Water Bay, Kowloon, Hong Kong, China
[61] Department of Physics, National Tsing Hua University, Hsinchu, Taiwan
[62] IJCLab, Université Paris-Saclay, CNRS/IN2P3, 91405 Orsay, France
[63] Department of Physics, Indiana University, Bloomington, IN, USA
[64] [(a)]INFN Gruppo Collegato di Udine, Sezione di Trieste, Udine, Italy; [(b)]ICTP, Trieste, Italy; [(c)]Dipartimento Politecnico di Ingegneria e Architettura, Università di Udine, Udine, Italy
[65] [(a)]INFN Sezione di Lecce, Lecce, Italy; [(b)]Dipartimento di Matematica e Fisica, Università del Salento, Lecce, Italy
[66] [(a)]INFN Sezione di Milano, Milan, Italy; [(b)]Dipartimento di Fisica, Università di Milano, Milan, Italy
[67] [(a)]INFN Sezione di Napoli, Naples, Italy; [(b)]Dipartimento di Fisica, Università di Napoli, Naples, Italy
[68] [(a)]INFN Sezione di Pavia, Pavia, Italy; [(b)]Dipartimento di Fisica, Università di Pavia, Pavia, Italy
[69] [(a)]INFN Sezione di Pisa, Pisa, Italy; [(b)]Dipartimento di Fisica E. Fermi, Università di Pisa, Pisa, Italy
[70] [(a)]INFN Sezione di Roma, Rome, Italy; [(b)]Dipartimento di Fisica, Sapienza Università di Roma, Rome, Italy
[71] [(a)]INFN Sezione di Roma Tor Vergata, Rome, Italy; [(b)]Dipartimento di Fisica, Università di Roma Tor Vergata, Rome, Italy

[72] [(a)]INFN Sezione di Roma Tre, Rome, Italy; [(b)]Dipartimento di Matematica e Fisica, Università Roma Tre, Rome, Italy
[73] [(a)]INFN-TIFPA, Povo, Italy; [(b)]Università degli Studi di Trento, Trento, Italy
[74] Institut für Astro- und Teilchenphysik, Leopold-Franzens-Universität, Innsbruck, Austria
[75] University of Iowa, Iowa City, IA, USA
[76] Department of Physics and Astronomy, Iowa State University, Ames, IA, USA
[77] Joint Institute for Nuclear Research, Dubna, Russia
[78] [(a)]Departamento de Engenharia Elétrica, Universidade Federal de Juiz de Fora (UFJF), Juiz de Fora, Brazil; [(b)] Universidade Federal do Rio De Janeiro COPPE/EE/IF, Rio de Janeiro, Brazil; [(c)]Instituto de Física, Universidade de São Paulo, São Paulo, Brazil
[79] KEK, High Energy Accelerator Research Organization, Tsukuba, Japan
[80] Graduate School of Science, Kobe University, Kobe, Japan
[81] [(a)]Faculty of Physics and Applied Computer Science, AGH University of Science and Technology, Kraków, Poland; [(b)] Marian Smoluchowski Institute of Physics, Jagiellonian University, Kraków, Poland
[82] Institute of Nuclear Physics Polish Academy of Sciences, Kraków, Poland
[83] Faculty of Science, Kyoto University, Kyoto, Japan
[84] Kyoto University of Education, Kyoto, Japan
[85] Research Center for Advanced Particle Physics and Department of Physics, Kyushu University, Fukuoka, Japan
[86] Instituto de Física La Plata, Universidad Nacional de La Plata and CONICET, La Plata, Argentina
[87] Physics Department, Lancaster University, Lancaster, UK
[88] Oliver Lodge Laboratory, University of Liverpool, Liverpool, UK
[89] Department of Experimental Particle Physics, Jožef Stefan Institute and Department of Physics, University of Ljubljana, Ljubljana, Slovenia
[90] School of Physics and Astronomy, Queen Mary University of London, London, UK
[91] Department of Physics, Royal Holloway University of London, Egham, UK
[92] Department of Physics and Astronomy, University College London, London, UK
[93] Louisiana Tech University, Ruston, LA, USA
[94] Fysiska Institutionen, Lunds Universitet, Lund, Sweden
[95] Departamento de Física Teorica C-15 and CIAFF, Universidad Autónoma de Madrid, Madrid, Spain
[96] Institut für Physik, Universität Mainz, Mainz, Germany
[97] School of Physics and Astronomy, University of Manchester, Manchester, UK
[98] CPPM, Aix-Marseille Université, CNRS/IN2P3, Marseille, France
[99] Department of Physics, University of Massachusetts, Amherst, MA, USA
[100] Department of Physics, McGill University, Montreal, QC, Canada
[101] School of Physics, University of Melbourne, Victoria, Australia
[102] Department of Physics, University of Michigan, Ann Arbor, MI, USA
[103] Department of Physics and Astronomy, Michigan State University, East Lansing, MI, USA
[104] B.I. Stepanov Institute of Physics, National Academy of Sciences of Belarus, Minsk, Belarus
[105] Research Institute for Nuclear Problems of Byelorussian State University, Minsk, Belarus
[106] Group of Particle Physics, University of Montreal, Montreal, QC, Canada
[107] P.N. Lebedev Physical Institute of the Russian Academy of Sciences, Moscow, Russia
[108] National Research Nuclear University MEPhI, Moscow, Russia
[109] D.V. Skobeltsyn Institute of Nuclear Physics, M.V. Lomonosov Moscow State University, Moscow, Russia
[110] Fakultät für Physik, Ludwig-Maximilians-Universität München, Munich, Germany
[111] Max-Planck-Institut für Physik (Werner-Heisenberg-Institut), Munich, Germany
[112] Graduate School of Science and Kobayashi-Maskawa Institute, Nagoya University, Nagoya, Japan
[113] Department of Physics and Astronomy, University of New Mexico, Albuquerque, NM, USA
[114] Institute for Mathematics, Astrophysics and Particle Physics, Radboud University/Nikhef, Nijmegen, The Netherlands
[115] Nikhef National Institute for Subatomic Physics and University of Amsterdam, Amsterdam, The Netherlands
[116] Department of Physics, Northern Illinois University, DeKalb, IL, USA
[117] [(a)]Budker Institute of Nuclear Physics and NSU, SB RAS, Novosibirsk, Russia; [(b)]Novosibirsk State University, Novosibirsk, Russia
[118] Institute for High Energy Physics of the National Research Centre Kurchatov Institute, Protvino, Russia

[119] Institute for Theoretical and Experimental Physics named by A.I. Alikhanov of National Research Centre "Kurchatov Institute", Moscow, Russia
[120] Department of Physics, New York University, New York, NY, USA
[121] Ochanomizu University, Otsuka, Bunkyo-ku, Tokyo, Japan
[122] Ohio State University, Columbus, OH, USA
[123] Homer L. Dodge Department of Physics and Astronomy, University of Oklahoma, Norman, OK, USA
[124] Department of Physics, Oklahoma State University, Stillwater, OK, USA
[125] Palacký University, Joint Laboratory of Optics, Olomouc, Czech Republic
[126] Institute for Fundamental Science, University of Oregon, Eugene, OR, USA
[127] Graduate School of Science, Osaka University, Osaka, Japan
[128] Department of Physics, University of Oslo, Oslo, Norway
[129] Department of Physics, Oxford University, Oxford, UK
[130] LPNHE, Sorbonne Université, Université de Paris, CNRS/IN2P3, Paris, France
[131] Department of Physics, University of Pennsylvania, Philadelphia, PA, USA
[132] Konstantinov Nuclear Physics Institute of National Research Centre "Kurchatov Institute", PNPI, St. Petersburg, Russia
[133] Department of Physics and Astronomy, University of Pittsburgh, Pittsburgh, PA, USA
[134] [(a)]Laboratório de Instrumentação e Física Experimental de Partículas-LIP, Lisbon, Portugal; [(b)]Departamento de Física, Faculdade de Ciências, Universidade de Lisboa, Lisbon, Portugal; [(c)]Departamento de Física, Universidade de Coimbra, Coimbra, Portugal; [(d)]Centro de Física Nuclear da Universidade de Lisboa, Lisbon, Portugal; [(e)]Departamento de Física, Universidade do Minho, Braga, Portugal; [(f)]Departamento de Física Teórica y del Cosmos, Universidad de Granada, Granada, Spain; [(g)]Dep Física and CEFITEC of Faculdade de Ciências e Tecnologia, Universidade Nova de Lisboa, Caparica, Portugal; [(h)]Instituto Superior Técnico, Universidade de Lisboa, Lisbon, Portugal
[135] Institute of Physics of the Czech Academy of Sciences, Prague, Czech Republic
[136] Czech Technical University in Prague, Prague, Czech Republic
[137] Charles University, Faculty of Mathematics and Physics, Prague, Czech Republic
[138] Particle Physics Department, Rutherford Appleton Laboratory, Didcot, UK
[139] IRFU, CEA, Université Paris-Saclay, Gif-sur-Yvette, France
[140] Santa Cruz Institute for Particle Physics, University of California Santa Cruz, Santa Cruz, CA, USA
[141] [(a)]Departamento de Física, Pontificia Universidad Católica de Chile, Santiago, Chile; [(b)]Universidad Andres Bello, Department of Physics, Santiago, Chile; [(c)]Instituto de Alta Investigación, Universidad de Tarapacá, Arica, Chile; [(d)] Departamento de Física, Universidad Técnica Federico Santa María, Valparaiso, Chile
[142] Universidade Federal de São João del Rei (UFSJ), São João del Rei, Brazil
[143] Department of Physics, University of Washington, Seattle, WA, USA
[144] Department of Physics and Astronomy, University of Sheffield, Sheffield, UK
[145] Department of Physics, Shinshu University, Nagano, Japan
[146] Department Physik, Universität Siegen, Siegen, Germany
[147] Department of Physics, Simon Fraser University, Burnaby, BC, Canada
[148] SLAC National Accelerator Laboratory, Stanford, CA, USA
[149] Department of Physics, Royal Institute of Technology, Stockholm, Sweden
[150] Departments of Physics and Astronomy, Stony Brook University, Stony Brook, NY, USA
[151] Department of Physics and Astronomy, University of Sussex, Brighton, UK
[152] School of Physics, University of Sydney, Sydney, Australia
[153] Institute of Physics, Academia Sinica, Taipei, Taiwan
[154] [(a)]E. Andronikashvili Institute of Physics, Iv. Javakhishvili Tbilisi State University, Tbilisi, Georgia; [(b)]High Energy Physics Institute, Tbilisi State University, Tbilisi, Georgia
[155] Department of Physics, Technion, Israel Institute of Technology, Haifa, Israel
[156] Raymond and Beverly Sackler School of Physics and Astronomy, Tel Aviv University, Tel Aviv, Israel
[157] Department of Physics, Aristotle University of Thessaloniki, Thessaloniki, Greece
[158] International Center for Elementary Particle Physics and Department of Physics, University of Tokyo, Tokyo, Japan
[159] Department of Physics, Tokyo Institute of Technology, Tokyo, Japan
[160] Tomsk State University, Tomsk, Russia
[161] Department of Physics, University of Toronto, Toronto, ON, Canada
[162] [(a)]TRIUMF, Vancouver, BC, Canada; [(b)]Department of Physics and Astronomy, York University, Toronto, ON, Canada

[163] Division of Physics and Tomonaga Center for the History of the Universe, Faculty of Pure and Applied Sciences, University of Tsukuba, Tsukuba, Japan
[164] Department of Physics and Astronomy, Tufts University, Medford, MA, USA
[165] Department of Physics and Astronomy, University of California Irvine, Irvine, CA, USA
[166] Department of Physics and Astronomy, University of Uppsala, Uppsala, Sweden
[167] Department of Physics, University of Illinois, Urbana, IL, USA
[168] Instituto de Física Corpuscular (IFIC), Centro Mixto Universidad de Valencia - CSIC, Valencia, Spain
[169] Department of Physics, University of British Columbia, Vancouver, BC, Canada
[170] Department of Physics and Astronomy, University of Victoria, Victoria, BC, Canada
[171] Fakultät für Physik und Astronomie, Julius-Maximilians-Universität Würzburg, Würzburg, Germany
[172] Department of Physics, University of Warwick, Coventry, UK
[173] Waseda University, Tokyo, Japan
[174] Department of Particle Physics and Astrophysics, Weizmann Institute of Science, Rehovot, Israel
[175] Department of Physics, University of Wisconsin, Madison, WI, USA
[176] Fakultät für Mathematik und Naturwissenschaften, Fachgruppe Physik, Bergische Universität Wuppertal, Wuppertal, Germany
[177] Department of Physics, Yale University, New Haven, CT, USA

[a] Also at Borough of Manhattan Community College, City University of New York, New York, NY, USA
[b] Also at Bruno Kessler Foundation, Trento, Italy
[c] Also at Center for High Energy Physics, Peking University, Beijing, China
[d] Also at Centro Studi e Ricerche Enrico Fermi, Rome, Italy
[e] Also at CERN, Geneva, Switzerland
[f] Also at Département de Physique Nucléaire et Corpusculaire, Université de Genève, Geneva, Switzerland
[g] Also at Departament de Fisica de la Universitat Autonoma de Barcelona, Barcelona, Spain
[h] Also at Department of Financial and Management Engineering, University of the Aegean, Chios, Greece
[i] Also at Department of Physics and Astronomy, Michigan State University, East Lansing, MI, USA
[j] Also at Department of Physics and Astronomy, University of Louisville, Louisville, KY, USA
[k] Also at Department of Physics, Ben Gurion University of the Negev, Beersheba, Israel
[l] Also at Department of Physics, California State University, East Bay, USA
[m] Also at Department of Physics, California State University, Fresno, USA
[n] Also at Department of Physics, California State University, Sacramento, USA
[o] Also at Department of Physics, King's College London, London, UK
[p] Also at Department of Physics, St. Petersburg State Polytechnical University, St. Petersburg, Russia
[q] Also at Department of Physics, University of Fribourg, Fribourg, Switzerland
[r] Also at Faculty of Physics, M.V. Lomonosov Moscow State University, Moscow, Russia
[s] Also at Faculty of Physics, Sofia University, 'St. Kliment Ohridski', Sofia, Bulgaria
[t] Also at Graduate School of Science, Osaka University, Osaka, Japan
[u] Also at Hellenic Open University, Patras, Greece
[v] Also at Institucio Catalana de Recerca i Estudis Avancats, ICREA, Barcelona, Spain
[w] Also at Institut für Experimentalphysik, Universität Hamburg, Hamburg, Germany
[x] Also at Institute for Particle and Nuclear Physics, Wigner Research Centre for Physics, Budapest, Hungary
[y] Also at Institute of Particle Physics (IPP), Victoria, Canada
[z] Also at Institute of Physics, Azerbaijan Academy of Sciences, Baku, Azerbaijan
[aa] Also at Institute of Theoretical Physics, Ilia State University, Tbilisi, Georgia
[ab] Also at Instituto de Fisica Teorica, IFT-UAM/CSIC, Madrid, Spain
[ac] Also at Department of Physics, Istanbul University, Istanbul, Turkey
[ad] Also at Joint Institute for Nuclear Research, Dubna, Russia
[ae] Also at Moscow Institute of Physics and Technology State University, Dolgoprudny, Russia
[af] Also at National Research Nuclear University MEPhI, Moscow, Russia
[ag] Also at Physics Department, An-Najah National University, Nablus, Palestine
[ah] Also at Physikalisches Institut, Albert-Ludwigs-Universität Freiburg, Freiburg, Germany
[ai] Also at The City College of New York, New York, NY, USA

[aj] Also at TRIUMF, Vancouver, BC, Canada
[ak] Also at Universita di Napoli Parthenope, Naples, Italy
[al] Also at University of Chinese Academy of Sciences (UCAS), Beijing, China
[am] Also at Physics Department, Yeditepe University, Istanbul, Turkey
* Deceased